Coordination Chemistry Reviews 253 (2009) 2814–2834

Contents lists available at ScienceDirect

Coordination Chemistry Reviews

journal homepage: www.elsevier.com/locate/ccr

Review

Magnetic lanthanide–transition-metal organic–inorganic hybrid materials: From discrete clusters to extended frameworks

You-Gui Huang, Fei-Long Jiang, Mao-Chun Hong*

Key Laboratory of Optoelectronic Materials Chemistry and Physics, Fujian Institute of Research on the Structure of Matter, Chinese Academy of Sciences, Fuzhou 350002, China

Contents

ARTICLE INFO

Article history:
Received 16 January 2009
Accepted 10 May 2009
Available online 27 May 2009

Keywords:
Lanthanide–transition-metal
Magnetic
Cluster
Framework
Slow relaxation
Hybrid

ABSTRACT

Magnetic lanthanide–transition-metal hybrid materials have enjoyed increasing attraction because they not only provide examples for studying magnetic coupling involving lanthanide ions but also exhibit novel magnetic behavior which render them candidates for future devices for information storage and quantum computation. Herein, we review the structures and magnetic properties of lanthanide–transition-metal hybrid materials that are categorized based on the structural features and organic ligands used. The review pays special attention to the examples which show magnetic slow relaxation since these render them to be potentially applied as devices for information storage.

1. Introduction

The chemistry of Ln–TM compounds (TM = transition metal) dates back almost a century. The origin can be traced to 1916, when a series of lanthanide hexacyanocobaltates $Ln[Co(CN)_6]\cdot n(H_2O)$ were synthesized [1a]. Up until now, numerous Ln–TM compounds have been obtained by various synthetic approaches [1].

* Corresponding author. Fax: +86 591 837914946.
E-mail address: hmc@fjirsm.ac.cn (M.-C. Hong).

0010-8545/$ – see front matter © 2009 Elsevier B.V. All rights reserved.
doi:10.1016/j.ccr.2009.05.007

In a recent review by Shore and coworkers, the existing Ln–TM compounds were summarized and a rational classification was proposed according to the different types of interactions between lanthanide and transition metal ions: (1) Ln–TM direct bonds, (2) ionic association, and (3) Ln-linkers-TM [2]. In particular, for the Ln-linkers-TM system, many examples were prepared from the aggregation of lanthanide, transition metal ions and diverse organic ligands due to the development of coordination chemistry and crystal engineering [3]. Research in this field has greatly progressed for the following reasons. First, the curiosity to synthesize new types of Ln–TM hybrid materials has encouraged creative synthetic strategies. Second, the Ln–TM heterometallic coordination complexes not only have attractive structure motifs but also important physical properties which render them candidates for luminescent sensors [4], catalysts [5], adsorption materials [6–8] and magnetic materials [9–12]. Finally, the magnetic Ln–TM hybrid materials provide abundant examples for studying the magnetic coupling involving lanthanide ions, a topic which is still far from being satisfactorily understood [12–20].

Studies of the magnetic interactions involving lanthanide ions were pioneered by Kahn and Gatteschi. In 1985, Gatteschi and coworkers observed that when Cu^{2+} and Gd^{3+} were bridged together, the coupling between the ions was ferromagnetic [21]. At that time, this result was surprising and aroused some skepticism as it might be expected that at least one of the seven 4f-orbitals would overlap with the semi-occupied orbital on Cu^{2+} which would result in an antiferromagnetic interaction between the two ions. Kahn and Gatteschi gave a rational explanation to the phenomenon [22,23]. Since the 4f-orbitals on lanthanide ions are small and internal, the interaction between the Cu^{2+} 3d and Gd^{3+} 4f orbitals is minimal, and hence the overlap is of little importance. The important interaction is between the orbital of $d_{x^2-y^2}$ on Cu^{2+} and an empty 5d-orbital on Gd^{3+}. In such a charge transfer configuration, there are two possible orientations for the electron transferred from Cu^{2+} to Gd^{3+}. One is that the additional electron aligns antiparallel to the seven 4f-electrons giving an $S = 3$ spin state equivalent to antiferromagnetic exchange; the other is that it aligns parallel to 4f-electrons leading to an $S = 4$ spin state equivalent to ferromagnetic exchange. According to Hund's rule, the latter will be lower in energy and hence the excited state of the system favors ferromagnetic exchange. After this pioneering work, many systems containing 4f–3d pairs of interacting ions were synthesized [24–28]. As to the exchange mechanism, most of the work focused on the nature of magnetic coupling involving Gd^{3+}, while that involving other lanthanide ions with large magnetic anisotropy is still not revealed mainly due to the unquenched orbital contribution which introduces many complications [13a]. Compared to the silence of the research on the exchange mechanism involving lanthanide ions, many Ln–TM hybrid materials with interesting magnetic properties have been obtained. For example, many discrete Ln–TM clusters showing magnetic slow relaxation have been reported [29,10b]; 4f–3d molecule-based magnets with high T_C (Curie temperature) have also been obtained [30]; Einaga and coworkers reported a cyano-bridged 3d–4f molecule-based magnet showing photoinduced magnetization which allows it to be used as a magnetic sensor [31].

We initiated our Ln–TM coordination complex research in the early 2000s. At that time several isolated Ln–TM clusters were reported [32], but Ln–TM complexes with extended structures were still very rare [33]. We aimed to synthesize Ln–TM coordination polymers with charming structures and interesting magnetic properties employing diverse synthetic strategies [34]. Gatteschi and coworkers reviewed the magnetic materials with interacting lanthanide and transition metal ions, and Winpenny et al. reviewed 3d–4f magnetic clusters [34d,e], herein we would like to review the structures and magnetic properties of Ln–TM hybrid materials. We classify these materials depending on their structural features (discrete and infinite in one, two and three dimensions, respectively). In particular, we pay special attention to compounds with novel magnetic properties.

2. Discrete clusters

As is well known, lanthanide ions have large and various coordination numbers and prefer to ligate to hard donor atoms, whereas d-block transition metal ions prefer to bind to soft donor atoms. This recognition of donor atoms by metal ions provides a potential approach to the synthesis of Ln–TM coordination complexes. However, to generate target Ln–TM compounds, a judicious choice of ligands is necessary. Except for cyano groups, multidentate ligands containing N-/O-donor atoms are considered good candidates and so are usually employed. Many Ln–TM compounds based upon multidentate N-/O-donor ligands have been prepared under diverse conditions [35–40].

Discrete Ln–TM clusters have been designed [42] from cyano groups, [31,41] ammonia phenol or carboxylic acids ligands. For example, Einaga and coworkers reported a cyano-bridged dinuclear Ln–TM compound showing photoinduced magnetization [31], and high nuclearity Ln–TM SMMs constructed from carboxylic acids ligands have also been obtained, but most of Ln–TM clusters are based on the following three kinds of ligands: Schiff-base [43–46], pyridonates [28,47–49] and amino acids [49–52].

2.1. Clusters using Schiff-base ligands

The magnetic interaction mechanism involving lanthanide and transition metal ions is one of the active issues in the study of discrete Ln–TM clusters, so special interest has been devoted to the synthesis of well-isolated dinuclear Ln–TM complexes to get direct information on the nature of the magnetic exchange. To avoid the problem of the unquenched orbital momentum of other lanthanide and transition metal ions, research interests mostly focus on the compounds containing Gd–Cu pairs. Due to the tendency of lanthanide ions towards high coordination numbers, the preparation of a simple dinuclear Ln–TM system usually requires specific ligands normally consisting of a N_2O_2 donor set. Several Schiff-base ligands with this character have been used to synthesize these dinuclear Ln–TM complexes [43–46,53]. The first fully characterized isolated dinuclear Gd-Cu compound $[L1CuGd(NO_3)_3]\cdot Me_2CO$ was synthesized by Costes et al. (L1 = 1,2-bis((3-methoxysalicylidene) amino)-2-methyl-propanato). In this molecule, the Cu^{2+} ion occupies the N_2O_2 compartment, while the Gd^{3+} ion enters the O_4 compartment, as in most of this type of systems [43–46,53]. The remaining coordination sites of the Gd^{3+} ion are occupied by counterions to furnish the eight-coordinate environment with distorted trigonal dodecahedron geometry. The Gd^{3+}–Cu^{2+} distance within the molecule is around 3.5 Å, while the intermolecular distance between paramagnetic centers is around 7–8 Å. The magnetic behavior of this dinuclear compound is characterized by the presence of a ferromagnetic Gd–Cu interaction. After analyzing a series of similar dinuclear systems, Costes et al. [54] proposed a correlation between the absolute value of the ferromagnetic coupling constant J and the exponential of the dihedral angle (c) between the two halves (Gd–O–Gd and O–Cu–O) of the bridging core: $|J| = A\exp(Bc)$, with $A = 11.5$, $B = -0.054$, $|J|$ (cm^{-1}), and c (°).

Employing different Schiff-base ligands, various Cu–Gd clusters including trinuclear Cu_2Gd complexes [21], tetranuclear Cu_2Gd_2 cages [12a], and hexanuclear $GdCu_5$ magnetic cores [55] have been observed. For instance, a trinuclear Cu_2Gd complex $[Cu_2Gd(L2)_2(HO_2)]\cdot(ClO_4)_3\cdot 2CuL2\cdot 0.5C_2H_5NO_2$ was syn-

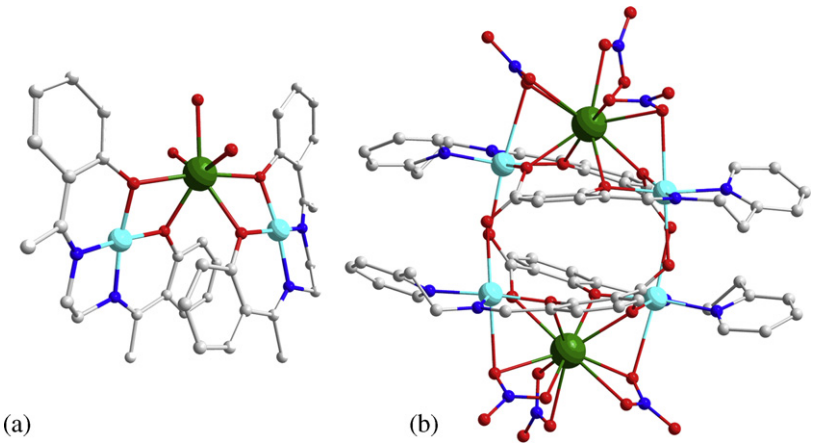

Fig. 1. (a) The trinuclear Cu_2Gd structure of $[Cu_2Gd(L2)_2(NO_3)_3]$ [21]; (b) the dimerisation of the trinuclear Cu_2Gd units $[Cu_4Gd_2(L3)_4(NO_3)_6]$ [12b].

thesized, whose asymmetric unit consists of three nuclear species where two Cu^{2+} ions are bonded to one Gd^{3+} ion by bridging oxygen atoms (L2 = *N*,*N*′-ethylenebis-(salicylaldiminato) [21] (Fig. 1a). Furthermore, a dimerization of the above trinuclear Cu_2Gd units $[Cu_4Gd_2(L3)_4(NO_3)_6]\cdot 0.5(CH_3OH\cdot H_2O)$ was also obtained by Kahn and coworkers (L3 is the ligand derived from 3-(*N*-2-(pyridylethyl)formimidoyl)salicylic acid) [12b] (Fig. 1b). In the Cu_4Gd_2 core, the Cu_2Gd subunits are connected through the carboxylate groups from L3 ligands to generate a hexanuclear Cu_4Gd_2 polyhedron which can be considered as a Cu_4 tetrahedron decorated with two Gd^{3+} ions. Notably, Luneau and coworkers reported a cubane $GdCu_3$ core and a Gd_3Cu_6 cluster resulting from the condensation of three $\{Gd_2Cu_2\}$ cubane-like moieties [12d]. Although some of these clusters present problems for the well-defined analysis of their magnetic properties, most magnetic studies supported the conclusion that the Cu–Gd coupling was ferromagnetic and the Cu–Cu and Gd–Gd exchanges were antiferromagnetic [59].

Due to the unquenched orbital momentum of Ni^{2+}, Co^{2+} and Cr^{3+} ions, it is difficult to quantitatively analyze the interactions of Gd^{3+}–Ni^{2+}, Gd^{3+}–Co^{2+}, and Gd^{3+}–Cr^{3+} pairs, so only a few reports on this research field are available in the literature. For the interactions of Gd^{3+}–Ni^{2+} pair, a dinuclear compound $[L4Ni(H_2O)_2Gd(NO_3)_3]$ containing a magnetically interacting Gd–Ni pair (L4 = [2,2′-[2,2′-dimethyl-1,3-propanediyl-bis(nitrilomethyldyne)]bis-(6-methoxyphenole)]) was reported. Magnetic studies suggest that the complex has a $S = 9/2$ ground state which derives from a Gd–Ni ferromagnetic interaction with a coupling constant of 3.6 cm^{-1} [44a]. Luo and coworkers also reported a heterodinuclear Gd–Ni cryptate with the presence of ferromagnetic interaction between the two metal ions ($J = 0.56\ cm^{-1}$) [56]. No clusters containing Gd^{3+}–Co^{2+} and Gd^{3+}–Cr^{3+} pairs were constructed from Schiff-base ligands, but such compounds constructed from other ligands were reported. For example, two dinuclear compounds including interacting Co^{2+}–Gd^{3+} pairs have been constructed from pivalate ligand or mixed ligands (pivalic acid and quinoline) [57,40]. In both cases, the authors concluded that the magnetic behavior may be ferromagnetic, but no quantitative analysis was done. In addition, a weak antiferromagnetic Gd^{3+}–Cr^{3+} interaction with $J = -0.09\ cm^{-1}$ was observed in the compound $[(acac)_2Cr(ox)Ln(HBpz_3)_2]$ (acac- = acetylacetonate, ox^{2-} = oxalate, $HBpz_3^-$ = hydrotris(pyrazol-1-yl)borate) [58].

Ferromagnetic Tb–Cu, Dy–Cu, Dy–Mn, Dy–Fe and Dy–Ni interactions were also observed in some Ln–TM clusters based on Schiff-base ligands. Due to the large magnetic anisotropy from Tb^{3+} and Dy^{3+} ions, these compounds may exhibit slow relaxation which is the characteristic of SMM (single molecule magnet). We will review these Ln–TM SMMs below.

2.2. Clusters constructed from pyridonates

Pyridonate molecules largely employed by Winpenny's group are also effective to construct high nuclearity Ln–TM clusters. Reaction of 2-pyridone with copper hydroxide and a hydrated lanthanoid nitrate gave the first such cluster $[Cu_4Gd_2(hp)_8(Hhp)_4(OH)_2(NO_3)_4(H_2O)_2]$ (Hhp = 2-pyridone) with Cu_4Gd_2 cage, where the six metal ions occupy the vertices of a distorted octahedron [25]. In this compound, the Cu_4Gd_2 core is besieged by twelve pyridonate ligands, eight of which link four Cu^{2+} ions into a cyclic tetranuclear subunit. If a 6-substuited 2-pyridonate is used, a series of predominantly tetranuclear Ln–TM cages can be obtained [28,47,49]. The lanthanide, solvent and pyridonate derivative influence the exact products of this series. Winpenny et al. classified these tetranuclear Ln–TM cages into two types. Type I features a central Cu_2O_2 ring, with two pyridonate ligands attached to each copper center through the N-donors of their rings, which further ligates to Ln atoms through the O-donors from pyridonate ligands. As a result, the Cu_2Ln_2 core is held by four pyridonate ligands. Type II has either Cu_3Ln or Cu_2Ln_2 core held by eight pyridonate ligands. Their structures have a similar arrangement of pyridonates, while the central rings are different, $CuLnO_2$ for Cu_3Ln core and Ln_2O_2 for Cu_2Ln_2 core, respectively (Fig. 2). Probably due to the larger radius of the La^{3+} ion, it has quite different coordination chemistry with the pyridonate ligands than the smaller 4f-elements. Some clusters seemingly unique to La centers, including Cu_4La_4 and Cu_3La cages, have been obtained [48]. Particularly, reaction of $[Cu_6Na(mhp)_{12}]\cdot NO_3$ with hydrated lanthanum nitrate in dichloromethane generated a fascinating highly ordered cluster $[Cu_{12}La_8(OH)_{24}(NO_3)_{21.2}(Hmhp)_{13}(H_2O)_{5.5}]\cdot[NO_3]_{2.8}$ (Hmhp = 6-methyl-2-pyridone) [60]. This cluster presents a central core incorporating a cuboctahedron of copper centers inside a cube of lanthanum, which implies the core has non-crystallographic O_h symmetry. The $Cu_{12}La_8$ core is exclusively held together by twenty-four μ_3-OH. Such a core can be assumed to consist of eight $LaCu_3$ tetrahedra with an OH group at the center of each $LaCu_2$ triangular face. Each copper is coordinated by four OH groups exhibiting a square plane geometry. The lanthanum centers are each bound by three μ_3-OH groups, with the remaining coordination sites furnished by different ligands, nitrate and water molecules. The La_8 and Cu_{12} cages show little distortion from the ideal polyhedron. For the La_8 cube, the La···La distances range from 6.301 to 6.705 Å and the Cu···Cu···Cu angles vary from 86.7° to 93.3°. The Cu···Cu contacts are invariant while the polyhedral angles deviate from 60° required for a perfect cuboctahedron. Surprisingly, if betaine ligands (either pyridinioacetate or pyridiniopropionate) are used,

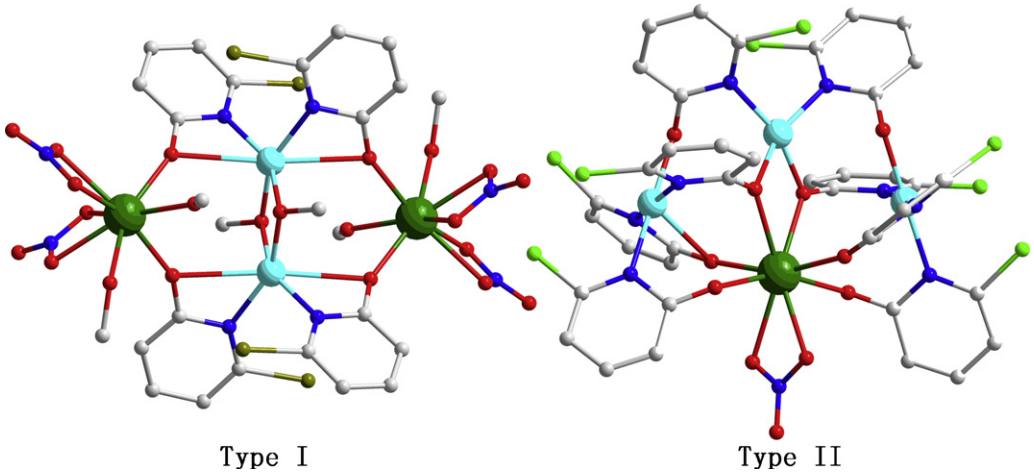

Fig. 2. Two types of tetranuclear Ln–TM cages based on 6-substituted 2-pyridonate [49].

a similar $Cu_{12}Ln_6(\mu_3\text{-}OH)_{24}$ (Ln = Y, Nd, Sm, Gd) cage, in which the cuboctahedron of copper centers remains unchanged from that of $Cu_{12}Ln_8(\mu_3\text{-}OH)_{24}$ core, can be isolated [61]. Rather than being coated in a Ln_8 cube, herein it is coated in a Ln_6 octahedron.

All the magnetic studies of these clusters reveal ferromagnetic interactions between Cu^{2+} and Gd^{3+} ions, which are in accordance with the initial observation. An empirical correlation between J and the Cu···Gd distance, $-J = A\exp[Bd_{Gd\cdots Cu}]$ (where $A = 6.5 \times 10^4$ and $B = -2.833$, with J in cm^{-1} and $d_{Gd\cdots Cu}$ in Å), has been proposed. However, due to the rather small range covered by these studies, this correlation still remains to be proven.

2.3. Clusters constructed from amino acids

Amino acids, because of their various coordination modes, have proven to be good candidates to construct high nuclearity clusters. Employing glycine, L-proline, L-alanine or L-threonine as ligands, Wu and coworkers synthesized a series of Ln–TM clusters including $\{LnM_6\}$, $\{Ln_6Cu_{12}\}$, $\{Ln_6Cu_{24}\}$, clusters, etc. [3e,62]. The self-assembly of $M(ClO_4)_2$ (M = Co, Ni), $Ln(ClO_4)_3$ (Ln = La, Pr) and amino acids (glycine, L-alanine, L-threonine) in aqueous media, generates a heptanuclear LnM_6 polyhedron $[NaLnM_6(AA)_{12}]\cdot(ClO_4)_4\cdot(H_2O)_{11}$ with a center coated Ln^{3+} ion (AA = glycine, L-proline, L-alanine or L-threonine) [62b]. In this polyhedron, twelve amino acids bridge the six M^{2+} ions into an octahedron, and each amino acid acts as an edge of the octahedron. The Ln^{3+} ion is located at the center of the octahedron coordinated by twelve oxygen atoms from twelve ligands. The structure is similar to that reported by Yukawa, which is constructed with L-prolinato [50]. A series of different LnM_6 clusters containing a Ln^{3+} center besieged in a trigonal prism formed by six Ni^{2+} metal ions were also synthesized [62c]. All the compounds in this system have a $[LnNi_6(gly)_6(\mu_3\text{-}OH)_3(H_2O)_6]^{6+}$ core and can be viewed as the edge ligands and/or terminal ligands exchange products of $[LnNi_6(gly)_6(\mu_3\text{-}OH)_3(H_2O)_6(\mu_2\text{-}H_2O)_3]^{6+}$. In theses compounds, two parallel layers being composed of three Ni^{2+} ions and three gly ligands nip the Ln^{3+} center together to form the final trigonal prism. Notably, another $\{LnM_6\}$ cluster $[LnCu_6(\mu_3\text{-}OH)_3(HIDA)_2(IDA)_4](ClO_4)_2\cdot 25H_2O$ with similar geometry was obtained by replacing glycine with iminodiacetate acid (HIDA) [63].

Two types of high nuclearity Ln–TM clusters $[Gd(H_2O)_8][Gd_6Cu_{12}(OH)_{14}(gly)_{15}(Hgly)_3(H_2O)_6]\cdot 16ClO_4\cdot 14H_2O$ $\{Gd_6Cu_{12}\}$ and $[Sm_6Cu_{24}(\mu_3\text{-}OH)_{30}(gly)_{12}(Ac)_{12}(ClO_4)(H_2O)_{16}]\cdot(ClO_4)_9\cdot(OH)_2\cdot(H_2O)_{31}$ $\{Sm_6Cu_{24}\}$ were also synthesized [62d,c]. The first features a crystallography imposed $\bar{3}$ symmetry and is composed of an isolated octadecanuclear cation $[Gd_6Cu_{12}(OH)_{14}(Gly)_{15}(HGly)_3(H_2O)_6]^{13+}$, an oct-aqua Gd^{3+} ion and several lattice water molecules (Fig. 3a). Six symmetry-related Gd^{3+} ions are bridged together by eight μ_3-OH groups to form a hollow octahedral Gd_6 core. On the other hand, two Cu^{2+} ions are linked to form a binuclear pair. Six such binuclear pairs encapsulate the Gd_6 core via μ_3-OH groups and glys, leading to the fan-shaped cation Gd_6Cu_{12}. The six Cu_2 binuclear units act as a blade and the Gd_6 cluster acts as the fan core. For the second cluster, the metal skeleton may be described as a large $\{Sm_6Cu_{24}\}$ octahedron encapsulated by twelve additional Cu^{2+} ions (every two connect to one Ln^{3+} vertex) with the help of μ_3-OH groups and glys (Fig. 3b). An encapsulated distorted ClO_4^- anion lies at the center of the $\{Sm_6Cu_{24}\}$ octahedron. Although a detailed study is still needed, the ClO_4^- anion seems to act as a template, which directs the formation of the large $\{Sm_6Cu_{24}\}$ cluster. In addition, some polydimensional supramolecular polymers based on $\{Ln_6Cu_{24}\}$ clusters can also be obtained by adjusting the reaction condition [64]. We will review these extended arrays below.

While using iminodiacetate acid as ligands, Long and coworkers obtained two highly sophisticated yet stunningly beautiful Ln–TM clusters $[La_{20}Ni_{30}(IDA)_{30}(CO_3)_6(NO_3)_6(OH)_{30}(H_2O)_{12}](CO_3)_6\cdot 72H_2O$ and $[Gd_{54}Ni_{54}(ida)_{48}(OH)_{144}(CO_3)_6(H_2O)_{25}](NO_3)_{18}\cdot 140H_2O$ [36a,65]. The cluster core of the first cluster features a keplerate type double-sphere structure with an inner sphere of 20 La^{3+} ions encapsulated by the outer sphere formed by 30 Ni^{2+} ions. The 30 Ni^{2+} ions construct an icosidodecahedron formed by 12 pentagonal and 20 triangular faces; while the 20 La^{3+} ions occupy the vertices of a perfect dodecahedron. The IDA ligands and μ_3-OH groups link the two metal spheres to form the final structure. Replacing the $La(NO_3)_3\cdot 6(H_2O)$ into $Gd(NO_3)_3\cdot 6(H_2O)$ in the reaction, a large four shell, nesting doll-like Ln–TM cluster was synthesized. Moving toward, the innermost shell (shell 1) contains six Ni^{2+} and two Gd^{3+} ions occupying the vertices of a cube and is followed by shell 2 of 20 Gd^{3+} ions occupying the vertices and the middle of the edge of a cube, by shell 3 with 32 Gd^{3+} ions forming a cube with two additional Gd^{3+} ions on each edge, and by the outermost shell (shell 4), a truncated cube with 48 Ni^{2+} ions, with each vertex being a triangle of Ni^{2+} ions.

Magnetic studies were carried out for most of these Ln–TM clusters based on amino acid ligands. Both ferromagnets and antiferromagnets were observed, but due to the crystal-field effects on the lanthanide ions and sophisticated structure of these clusters, it is difficult to quantify the individual contributions of the transition metal and lanthanide ions. As far as we know, there is only one cluster $[Gd(H_2O)_8][Gd_6Cu_{12}(OH)_{14}(gly)_{15}(Hgly)_3(H_2O)_6]\cdot 16ClO_4\cdot 14H_2O$ $\{Gd_6Cu_{12}\}$ whose magnetic susceptibility was quantitatively analyzed. The

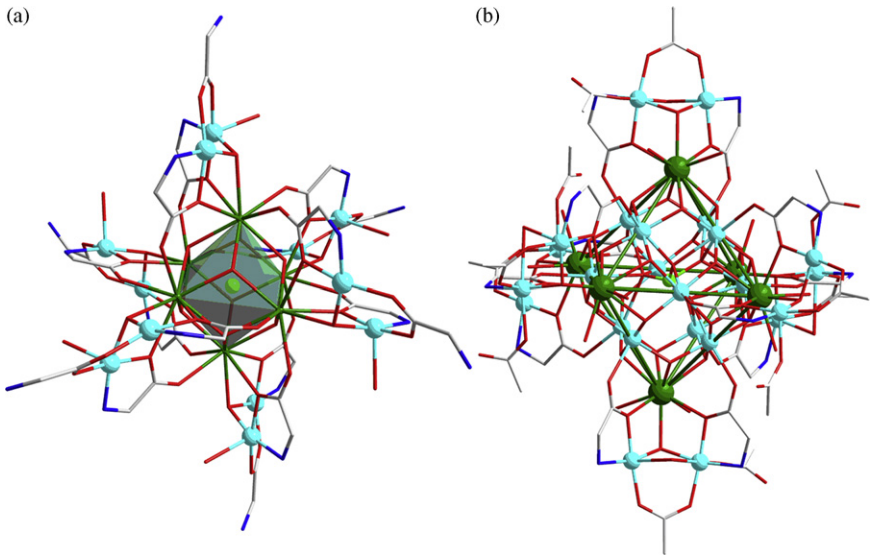

Fig. 3. (a) The fan-shape $\{Gd_6Cu_{12}\}$ cluster structure [62d]; (b) the glc bridged $\{Sm_6Cu_{24}\}$ cluster [62c].

best fit was found with $J_{Gd-Gd} = 0.0016\,cm^{-1}$, $J_{Gd-Cu} = 9.6\,cm^{-1}$ and $J_{Cu-Cu} = -857.3\,cm^{-1}$. Unfortunately, in spite of the large cluster structure, there is no magnetic slow relaxation observed for any of these complexes.

2.4. Ln–TM single molecular magnet

Some metal ions with large magnetic anisotropy are considered to be good candidates for synthesizing magnetic materials with interesting behavior. The most important of these magnetic materials is the single molecule magnet (known as SMM) which is associated with the combined effect of a ground state with high-spin value (S), easy axis anisotropy ($D < 0$, in which D is defined as the zero-field splitting parameter), and small transverse anisotropy. It follows Arrhenius law with a characteristic energy gap Δ for reversal between up-spin and down-spin given roughly by $\Delta = |D|S^2$. Slow relaxation is observed at low temperature when $|D|S^2 \gg k_BT$. A large J/J' ratio (in which J is the intramolecular exchange interaction and J' the intermolecular exchange interaction) is also required to observe SMM behavior [29b].

Recently, the field of SMM has extended into well-isolated discrete Ln–TM clusters in which highly anisotropy lanthanide ions are usually employed. The Ln–TM SMMs reported are mainly high nuclearity clusters involving highly anisotropic Tb^{3+} or Dy^{3+} ions. Various multidentate ligands have been employed, including Schiff-base ligands, carboxylic acids and alcohol ligands.

There are a few reports on Ln–TM SMMs based upon Schiff-base ligands. Most of them are constructed from Dy^{3+} ion, except a cyclic $Cu^{2+}{}_2Tb^{3+}{}_2$ SMM $[Cu^{2+}L5Tb^{3+}(hfac)_2]_2$ in which the molecule has an inversion center and the Cu^{2+} and Tb^{3+} ions are arrayed alternately (H_3L5 = 1-(2-hydroxybenzamido)-2-(2-hydroxy-3-methoxy-benzylideneamino)-ethane, Hhfac = hexafluoroacetylacetone) [3b]. The Cu···Cu and Tb···Tb distances are around 4.9 and 7.9 Å, respectively, indicating that each ion pair is well separated. Furthermore, the cyclic tetranuclear molecules are well isolated in the crystal and the compound can be described as a magnetically isolated molecule. The magnetic susceptibility measurement reveals a ferromagnetic interaction between the Tb–Cu pairs. Further magnetic characterizations show that this cluster exhibits SMM behavior which is confirmed by the concomitant appearance of an out-of-phase signal. The out-of-phase component of the ac susceptibility χ''_m shows frequency dependent peaks at around 2.5 K. Fitting the data by Arrhenius law, the obtained best fitting parameters are $\hat{o}_0 = 2.7 \times 10^{-8}$ s and $\Delta/k_B = 21$ K, and the estimated T_B is 1.2 K.

The structures of Ln–TM magnets showing slow relaxation based upon Schiff-base ligands containing Dy^{3+} ions vary considerably including linear $\{Dy_2Cu\}$, $\{Dy_3Cu_6\}$, planar $\{DyCu_5\}$ and $\{Dy_6Mn_6\}$ cores [2b,2c,13a,29b]. For instance, very recently, Gatteschi and coworkers reported two linear Dy_2M trinuclear compounds $[\{Dy(hfac)_3\}_2\{Fe(bpca)_2\}]\cdot CHCl_3$ and $[\{Dy(hfac)_3\}_2\{Ni(bpca)_2\}]\cdot CHCl_3$ ($bpca^-$ = bis(2-pyridylcarbonyl) amine anion) [29b]. In both compounds, a central $[M(bpca)_2]$ ($M = Fe^{2+}$, Ni^{2+}) unit is linked to two terminal $[Dy(hfac)_3]$ units. Static magnetic susceptibility measurements reveal a weak ferromagnetic exchange interaction between Ni^{2+} and Dy^{3+} ions, while the diamagnetic Fe^{2+} ion leads to the absence of magnetic interaction. Dynamic susceptibility measurements show a thermally activated behavior with the energy barrier of 9.7 and 4.9 K, respectively. Thanks to the comparison of the magnetic behavior of these two compounds, an interesting negative effect of the ferromagnetic exchange interaction on the dynamics of the magnetization has been found. Ishida and coworkers also reported a similar linear compound $[\{Dy(hfac)_3\}_2\{Cu(dpk)_2\}]$ with $\{Dy_2Cu\}$ core with $\hat{o}_0 = 1.5 \times 10^{-7}$ s and $\Delta/k_B = 47$ K showing interesting quantum tunneling of magnetization (Hdpk = di-2-pyridyl ketoximate) [13a]. By employing the "one-step strategy", Pecoraro and coworkers can obtain a large $\{Dy_6Mn_6\}$ cluster $[Dy_6Mn_6(H_2L6)_4(HL6)_2(L6)_{10}(CH_3OH)_{10}(H_2O)_2]\cdot 9CH_3OH\cdot 8H_2O$ showing SMM behavior (H_2L6 = salicylhydroxamic acid) [3c]. This cluster is centered about a nearly planar hexagonal ring of Dy^{3+} ions that is capped on either end by a $Mn_2{}^{3+}Mn^{4+}$ trimer. In a word, sixteen L6 ligands ligate the six Dy^{3+} ions and six manganese ions together to form the large condensed cluster (Fig. 4). Upon cooling, the χ_mT value decreases continuously, which is indicative of dominant intramolecular antiferromagnetic exchange interaction in the cluster, depopulation of dysprosium single-ion sublevels, or a combination of both. However, the ac magnetic measurements reveal its SMM behavior, for a frequency dependent out-of-phase component (χ''_m) signal appears. Unfortunately, due to the low blocking temperature ($T_B < 2$ K), no relaxation time $\hat{o}_0$ and energy barrier Δ/k_B was reported.

Simple monocarboxylic acids ligands have also been employed to construct Ln–Mn SMMs by Christou's group and Powell's

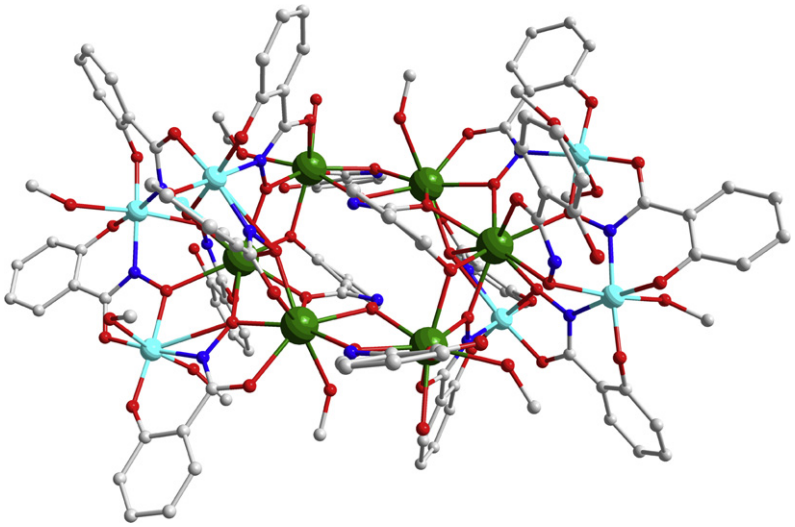

Fig. 4. The core structure of $\{Dy_6Mn_6\}$ cluster showing slow relaxation [3c].

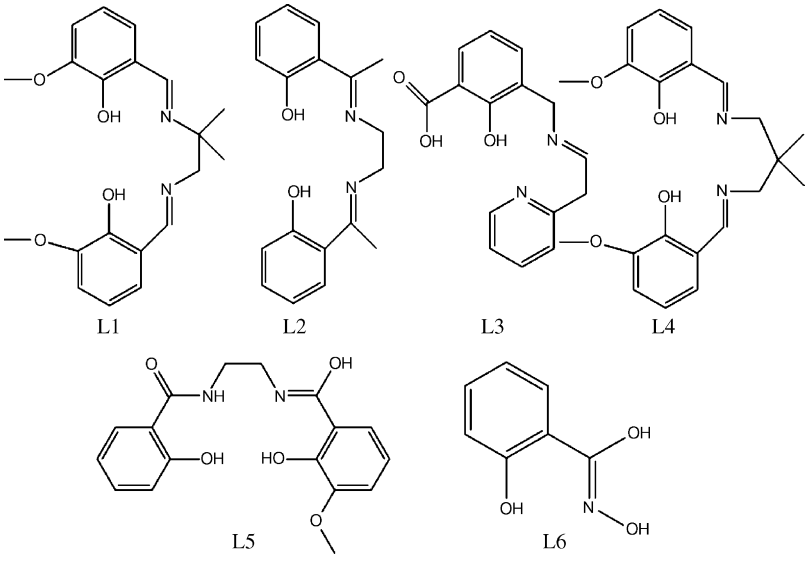

Scheme 1. Schiff-base ligands used to construct Ln–TM clusters appearing in this review.

group. Employing $^tBuCO_2H$, Powell and coworkers isolated a bell-shaped $\{Gd_2Mn_{11}\}$ cluster and a $\{Ln_4Mn_5\}$ (Ln = Tb, Dy, Ho, Y) cluster with central core composed of two distorted $\{Ln_2Mn_2O_4\}$ cubanes sharing a Mn^{4+} vertex [29c,g]. Both of these Ln–Mn clusters unambiguously exhibit SMM behavior and the $\hat{o}_0$, Δ/k_B for the bell-shaped $\{Gd_2Mn_{11}\}$ cluster $[Mn^{3+}{}_9Mn^{2+}{}_2Gd_2(O)_8(OH)_2(piv)_{10.6}(fca)_{6.4}(NO_3)_2(H_2O)]\cdot 13CH_3CN\cdot H_2O$ are 2×10^{-12} s and 18.4 K, respectively (Hfca = 2-furan-carboxylic acid, Hpiv = $^tBuCO_2H$). Combination $^tBuCO_2H$ and H_3tmp, Brechin and coworkers obtained a cyclic $\{Dy_2Mn_2\}$ cluster $[NMe_4]_2[Mn_2Dy_2(tmp)_2(O_2CCMe_3)_4(NO_3)_4]\cdot 2MeCN\cdot 0.5H_2O$ showing not only frequency dependent out-of-phase ac susceptibility signals but also temperature and sweep rate dependent hysteresis loops (H_3tmp = propane-1,1,1-triol) [29f]. While using $PhCO_2H$, Christou and coworkers synthesized two large Ln–Mn clusters with $\{Dy_4Mn_{11}\}$ or $\{GdMn_{12}\}$ cores, both showing interesting quantum tunneling of magnetization (QTM) [29d,h]. For the $\{GdMn_{12}\}$ cluster, clear quantum tunneling steps can be observed in its hysteresis loops (Schemes 1 and 2).

3. Extended arrays

3.1. Synthesis strategy

Over the last 20 years, the tremendous development of functional hybrid materials has greatly stimulated the synthesis of Ln–TM coordination polymers. Apart from the aesthetic perspective, the interest in such polymers arises from their novel properties and potential applications as magnetic materials [66], photoluminescent materials and zeolite-like materials [67]. For instance, using the molecular precursor $[Cu(opba)]^{2-}$, Kahn obtained a series

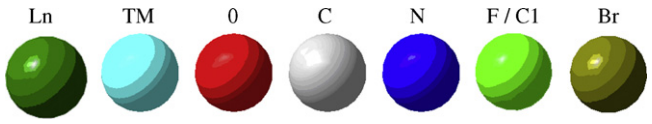

Scheme 2. Key for figures in this review.

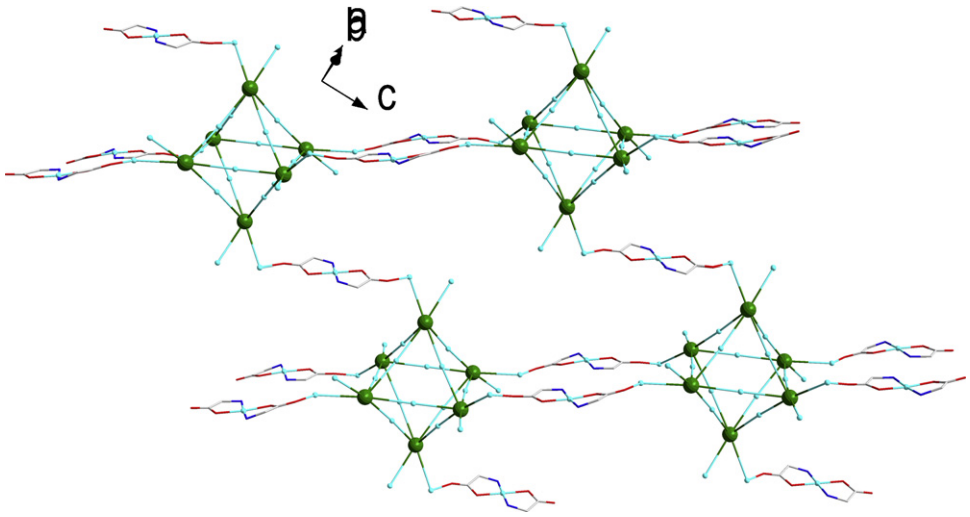

Fig. 5. The 2D (4, 4) net-like structure of $Na_2[Ln_6Cu_{27}(gly)_{20}(\mu_3\text{-}OH)_{30}(H_2O)_{22}(ClO_4)](ClO_4)_{23}(H_2O)_{28}$ based on $\{Ln_6Cu_{24}\}$ cluster [64].

of 3d–4f multidimensional magnetic materials showing different long-rang magnetic ordering [6]; Cheng and coworkers developed a luminescent probe of Zn^{2+} ions with porous zeolite-type structure [4a,67]. On the other hand, the search for new synthetic routes leading to functional 3d–4f hybrids is also a focus of research for chemists, physical scientists and material scientists. By manipulating the various forces in order to design target 3d–4f coordination polymers with useful properties, chemists have realized that the resulting structures are determined by the following factors: (1) metal-to-ligand stoichiometry, (2) the stereochemical preference of the assembling cations, (3) the use of ancillary ligands, (4) the intervention of the noncovalent interactions (hydrogen bonds, π–π stacking interactions), (5) the role of the anions (coordinated, bridging, uncoordinated), and (6) the presence of organic guest molecules, which can act as templates [68]. Several rational synthetic approaches aiming at obtaining heterometallic Ln–TM polymers have been proposed and developed. The most direct way is reaction of lanthanide salts, transition metal salts and organic links in one step, and most of the reported 3d–4f polymers have been prepared by this strategy [34,67,69]. The approach based on heterometallic Ln–TM cluster as nodes has also proven to be effective to construct 3d–4f hybrids [68,70]; the metalloligand approach is also used, that is self-assembly process involving metalloligands and diverse lanthanide cations [71,72]; recently a new approach which introduces the cooperation of different organic ligands has been developed [73]. For our own work, using the polycarboxylic acids as ligands and employing various strategies, we obtained series of 3d–4f coordination polymers containing materials which feature aesthetic structures and interesting properties [3a,e,34,74]. Here we will review the Ln–TM coordination polymers according to their structural features.

3.2. Extended frameworks based on Ln–TM clusters or metalloligands

3.2.1. Extended frameworks based on Ln–TM clusters

In contrast to the fruitful production of extended frameworks based on transition-metal clusters, those based on Ln–TM clusters are still very scarce [70]. The use of metal clusters to construct extended arrays can not only make the functional frameworks inherit interesting magnetic, optical and electrical properties from the clusters introduced, but also make the size of caves or pores of coordination polymers increase, which is of great significance for the design and synthesis of frameworks analogous to important minerals such as quartz, clays and zeolites [75]. Some porous frameworks based transition metal or lanthanide clusters have been observed which exhibit both novel magnetic and adsorption properties known as porous magnets [76]. However, this area corresponding to Ln–TM clusters still remains to be explored.

As discussed above, employing amino acids, Wu and coworkers obtained a series of high nuclearity Ln–TM clusters. With the help of *trans*-$Cu(gly)_2$ or *trans*-$Cu(Pro)_2$ unit and by adjusting the reaction conditions, both 2D and 3D coordination polymers based on Ln_6Cu_{24} clusters can be obtained [64,70b]. With the help of *trans*-$Cu(gly)_2$, a 2D compound with formula $Na_2[Ln_6Cu_{27}(gly)_{20}(\mu_3\text{-}OH)_{30}(H_2O)_{22}(ClO_4)](ClO_4)_{23}(H_2O)_{28}$ (Ln = Er, Eu, Gd), was obtained (Fig. 5). In this compound, Ln_6Cu_{24} clusters are first double bridged by two *trans*-$Cu(gly)_2$ linkers to generate a 1D chain running along the crystallography *b*-axis. Then these chains are further connected together by *trans*-$Cu(gly)_2$ units. That is, each Ln_6Cu_{24} cluster is connected to four neighboring ones by six *trans*-$Cu(gly)_2$ units, resulting in a 2D net-like framework with (4, 4) topology. Two 3D compounds based on $\{Ln_6Cu_{24}\}$ clusters $\{[Sm_6Cu_{29}(i_3\text{-}OH)_{30}(gly)_{24}(ClO_4)(H_2O)_{22}](ClO_4)_{14}\cdot(OH)_7\cdot(H_2O)_{24}\}_n$ and $\{[Nd_6Cu_{30}(\mu_3\text{-}OH)_{30}(Pro)_{24}(ClO_4)(H_2O)_{21}]\cdot(ClO_4)_{12}\cdot(OH)_{11}\cdot(H_2O)_6\}_n$ can also be synthesized with the help of *trans*-$Cu(gly)_2$ or *trans*-$Cu(Pro)_2$ unit, respectively. For the first compound, each Sm_6Cu_{24} unit is connected via ten *trans*-$Cu(gly)_2$ groups to six neighboring ones to give rise to a 3D porous network with quasi-rectangular 7 Å × 31 Å channels along *b*-axis. According to topology approach, the net can be simplified as α-Po net with $(4^9\cdot6^6)$ Schläfli symbol. In the second compound, differently, each Ln_6Cu_{24} cluster is connected to twelve adjacent ones by twelve *trans*-$Cu(Pro)_2$ bridges to generate a 3D framework. Notably, each *trans*-$Cu(Pro)_2$ unit attaches two Cu^{2+} ions from different clusters. The complicated 3D framework can be described as a 12-connected *fcu* net. In other words, the 3D structure can also be considered to be constructed from interlinked $\{Nd_6Cu_{24}\}_{13}$ dodecahedral cages coating a Nd_6Cu_{24} cluster center. This $\{Nd_6Cu_{24}\}_{13}$ dodecahedron cage not only has large pores itself, but also can form superlattices with large pore size and high pore volume. Remarkably, Chen et al. also successfully extended their $\{Ln_6Cu_{24}\}$ clusters into a 2D structure [70b]. Magnetic studies for all these compounds indicate that all of them behave as antiferromagnets, but it is difficult to clearly determine the nature of magnetic interactions involving the metal ions.

Costes and coworkers also reported a series of extended arrays based on dinuclear or trinuclear cluster units constructed from a Schiff-base ligand (L4) (Fig. 6) [68]. Different from Wu's compounds based on metalloligand bridged $\{Ln_6Cu_{24}\}$ clusters, two families

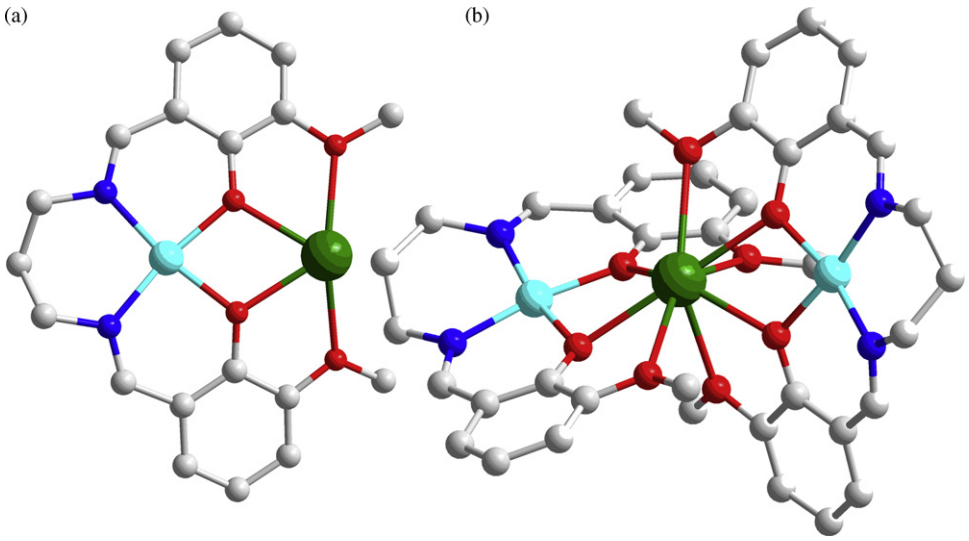

Fig. 6. The dinuclear (a) and trinuclear (b) cluster units in the series of compounds obtained by Costes and coworkers [68].

of bridges have been employed as linkers in the system: the first consists of *exo*-dentate ligands bearing nitrogen donor atoms such as bipyridine (bipy) and dicyanamido (dca), while the second consists of *exo*-dentate ligands with oxygen donor atoms containing anions derived from the acetylenedicarboxylic (H_2acdca), fumaric (H_2fum), trimesic (H_3trim) and oxalic (H_2ox) acids. Interestingly, the nature of linkers shows an important impact on the final structural diversity. Using bipy as linker, as expected, two {CuLn} entities are bridged together leading to a tetranuclear complex. However, the ligands belonging to the second family connect the cluster units into extended arrays. Using H_2acdca linkers, the {CuLn} entities are alternatively bridged by one or two acdca ligands into a zigzag chain. The H_2fum can link the {CuLn} entities into a single chain, double chain or 2D brick-wall type layer with (6, 3) net, and the H_3trim connects the {CuLn} entities into a double chain. H_2ox cooperation with 2,2′-bipy connects {CuLn} entities into a zigzag chain, while if H_2ox cooperates with dca, trinuclear {Cu_2Ln} entities were extended into honeycomb layer. For all of the compounds involving Gd^{3+} ions, the Cu^{2+}–Gd^{3+} exchange interaction were ferromagnetic, with J values in the range of 3.53–8.96 cm^{-1}. Due to the depopulation of the Stark levels of other lanthanide ions, the nature of the magnetic exchange involving them is unclear.

3.2.2. Extended frameworks based on metalloligands

The metalloligand approach, which is also called stepwise synthesis, has been employed to construct multidimensional Ln–TM structures in the past few years. Generally, the metalloligand should be relatively stable and contain potential coordinating atoms. Several metalloligands have proven to be effective and a variety of Ln–TM compounds were synthesized.

Kahn and coworkers reported a honeycomb ferromagnet using Na_2[Cu(pba)] as a metalloligand [72]. Yan and coworkers designed a bifunctional ligand HL7 (Scheme 3a) that contains two different coordination sites: lanthanide ions will interact with the pyridine-N-oxide, while the transition metal ions will bind to a tridentate chelating site [71a]. As expected, an orthogonal metalloligand Ni(HL7)L7ClO_4 can first be isolated, and employing this, an extended 1D Ln–Ni chain with formula {$LnNi_2L_3$(HL7)$(DMF)_4(ClO_4)_4$·S} (Ln = Gd, Tb, S = solvent) can be obtained. In the chain, two adjacent Ln^{3+} ions and two bridging metalloligands form a square unit, and these units are linked together by sharing the common Ln^{3+} nodes. For the Gd derivative, as the temperature is lowered, the χT first decreases slowly, reaching a minimum at ca. 64 K, and then increases reaching a maximum at ca. 12 K, and then decreases dramatically. This phenomenon indicates that the complex behaves as a ferromagnetic chain with antiferromagnetic interactions between the adjacent paramagnetic centers with uncompensated spins.

Using the metalloligand Cu(pic)$_2$ (Scheme 3b), Guo and coworkers synthesized a series of Ln–Cu coordination polymers, containing linear chain {$NdCu(pic)_2[CO(NH_2)_2]_4(H_2O)_3$}$(ClO_4)_3$·[Cu(pic)$_2$]$_2$, zigzag chain [$LnCu_2(pic)_4(H_2O)_6$]$(ClO_4)_3$·$H_2O$ (Ln = Sm, Nd, and Pr) and a 2D layer structure constituted by Cu(pic)$_2$ moiety bridged zigzag chains with formula [$Ln_2Cu_5(pic)_{10}(H_2O)_8$]$(ClO_4)_6$·$2H_2O$ (Ln = Gd, Nd, Sm, Dy, Eu, Pr, and Yb Hpic = picolinic acid) [71b]. Although magnetic data were collected for some of the compounds in this system, due to the progressive thermal depopulation of the Ln^{3+} Stark components, the nature of Ln^{3+}–Cu^{2+} interactions remains to be clarified.

As for our own work, we developed a new metalloligand [Co(2,5-Hpydc)$_3$]·$3H_2O$ (Scheme 3c), in which the Co^{3+} is octahedrally coordinated with three N and three O atoms from three 2,5-Hpydc moieties (2,5-H_2pydc = 2,5-pyridine dicarboxylic acid) [74g]. The metalloligand [Co(2,5-pydc)$_3$]$^{3-}$ has two kinds of Lewis-base coordination groups, 2-carboxylate group (group A) and 5-carboxylate group (group B) moieties. The bridging capability of group A is weaker than that of group B because of its weak electron-donating and electro static power, and the distance between adjacent groups B is considerable larger which allows [Co(2,5-pydc)$_3$]$^{3-}$ to form well isolated magnetic nanowires. In this regard, [Co(2,5-pydc)$_3$]$^{3-}$ may be a better candidate for single chain magnets (SCMs) than the original 2,5-H_2pydc if the control of the choice of metal ions for coordination

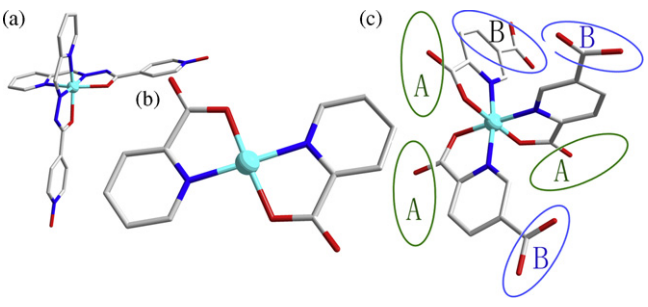

Scheme 3. (a) The metalloligand of [Ni(HL7)L7]$^+$; (b) the metalloligand of Cu(pic)$_2$; (c) the metalloligand of [Co(2,5-pydc)$_3$]$^{3-}$ [74g].

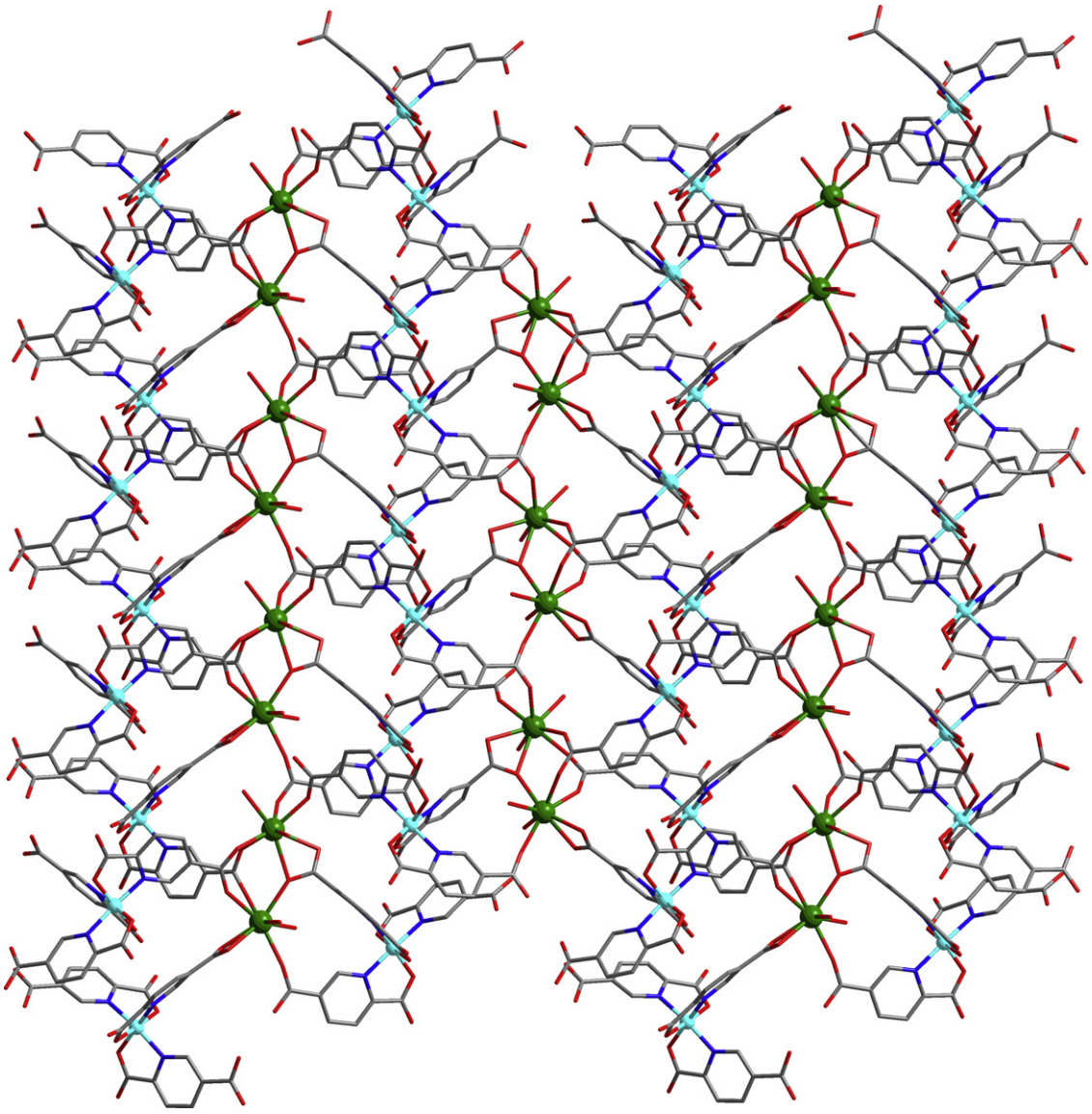

Fig. 7. The 2D layer structure of $[Dy_2Co_2(2,5\text{-pydc})_6(H_2O)_4]_n{\cdot}2nH_2O$ [74g].

groups is possible. Indeed, using metalloligand $[Co(2,5\text{-pydc})_3]^{3-}$ to covalently link lanthanide ions into an extended network, we obtained four cobalt-lanthanide heterometallic compounds $[Dy_2Co_2(2,5\text{-pydc})_6(H_2O)_4]_n{\cdot}2nH_2O$, $[Tb_2Co_2(2,5\text{-pydc})_6(H_2O)_4]_n{\cdot}3nH_2O$, $[Tb_2Co_2(2,5\text{-pydc})_6(H_2O)_9]_n{\cdot}4nH_2O$ and $[LaCo(2,5\text{-pydc})_3(H_2O)_2]_n{\cdot}2nH_2O$, some of them exhibit interesting like-SCM behavior.

In the first compound, the Ln^{3+} ions are first bridged into a chain by carboxylate groups from metalloligand $[Co(2,5\text{-pydc})_3]^{3-}$, which is further extended leading to a layer with large inter chain Dy···Dy distances (Fig. 7). For the second compound, there are two crystallographic unique metalloligands $[Co(2,5\text{-pydc})_3]^{3-}$ in its asymmetric unit. One links the Tb^{3+} ions into a layer based upon linear carboxylate-bridged $[Tb^{3+}]_4$ units, the other bridges the Tb^{3+} ions into a tape which is based upon linear carboxylate-bridged $[Tb^{3+}]_4$ units. The tapes interlinked with layers above by sharing Tb^{3+} ions to generate a porous three-dimensional network, resulting from the $[Tb^{3+}]_4$ units bridged by carboxyl groups to form a carboxylate-bridged Tb^{3+} chain. In the 3D network, each carboxylate-bridged Tb^{3+} chain connects with four other adjacent chains with an interchain $Tb^{3+}\cdots Tb^{3+}$ distance of about 13 Å. For the third compound, one crystallographic unique metalloligand connects the Tb^{3+} ions into a chain formed by two kinds of dimers, the other links the chains into a layer structure with the shortest interchain $Tb^{3+}\cdots Tb^{3+}$ distance 7.470 Å. The fourth compound is an intricate 3D architecture, which can be viewed as a uninodal 5-connected net with boron nitride (BN) topology and $(4^3{\cdot}5{\cdot}6^5{\cdot}8)$ Schäfli symbol.

Temperature-dependent magnetic susceptibility measurements for the former two compounds reveal that notable ferromagnetic interactions exist in the carboxylate-bridged Ln^{3+} chains, while the $Tb^{3+}\cdots Tb^{3+}$ magnetic interaction in the third compound may be antiferromagnetic. The ferromagnetic interactions in the carboxylate-bridged Ln^{3+} chains were further confirmed by their M vs H curves which show fast-saturation variations. For the observed ferromagnetic coupling between Ln^{3+} ions in the carboxylate-bridged chains, we measured the ac magnetic susceptibility in zero applied dc field. The linear variation of $\ln(\chi'_m T)$ versus T^{-1} observed indicates a strong Ising-like chain. No irreversibility was observed in the ZFC and FC magnetization, thereby indicating no long-range order, which further confirms their 1D nature. No clearly frequency-dependent out-of-phase signal was observed for the second compound above 2 K, which excludes the possibility that it exhibits single-chain magnet behavior. However,

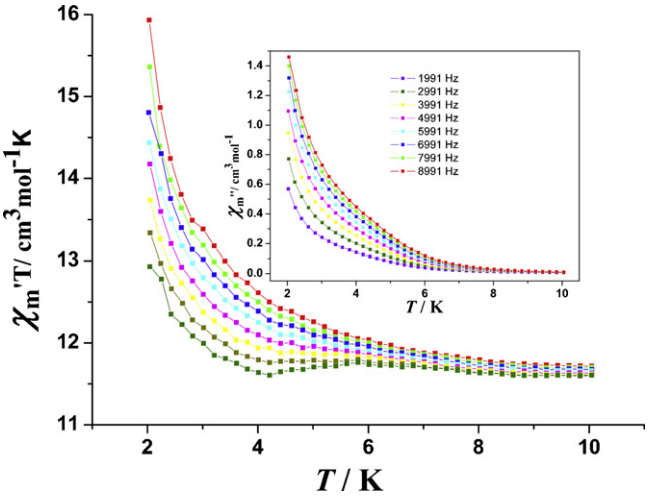

Fig. 8. Temperature dependence of ac χ_m at different frequencies for $[Dy_2Co_2(2,5\text{-pydc})_6(H_2O)_4]_n{\cdot}2nH_2O$ [74g].

both clearly frequency-dependent in-phase and out-of-phase signals were observed for the first compound (Fig. 8). This behavior is a proof for the SCM, although it does not mean it is definitely a SCM, since spin-glass or random-domain magnets can also lead to such signals. To further investigate this behavior, isothermal frequency-dependent ac susceptibility of the first compound was measured to evaluate the effective energy barrier and relaxation time. The data were fitted by a generalized Debye model. The $\hat{o}$ values obtained are further used and fitted by the Arrhenius law [$\hat{o} = \hat{o}_0 \exp(U_{eff}/k_BT)$], giving $\acute{a} \approx 0.18$, $U_{eff} = 4.89$ K, $\hat{o}_0 = 7.56 \times 10^{-8}$ s, indicating a narrow distribution of relaxation times. An ideal SMM or SCM is likely to possess a single relaxation time ($\acute{a} = 0$) whereas a spin glass would show a wide range of relaxation process ($\acute{a} = \rightarrow 1$). The $\acute{a}$, U_{eff} and $\hat{o}_0$ values obtained allow us to assess that we are not faced with a spin glass behavior and the values are comparable to those of some other SCMs or SMMs.

3.3. One-dimensional Ln–TM materials

One-dimensional compounds, especially the simple chain structures, comprising lanthanide ions and transition metal ions are exceedingly rare. For the reported compounds, cyano, CCl_3COO^-, H_2pydc, oxalate, opba (*o*-phenlenebis(oxamato)) as well as bpa (2-hydroxy-l,3-propylenebis(oxamato)) were employed.

$[M(CN)_6]^{3-}$ ions (M = Fe, Mn, Cr) show a great capability to bridge lanthanide ions, so they are considered to be good candidates to construct Ln–TM compounds. Indeed, a series of simple 1D chain structures were synthesized by using $[M(CN)_6]^{3-}$ ions as precursors [77]. For the compounds in this system, the $[M(CN)_6]^{3-}$ ion can use its two cyano groups to ligate to Ln^{3+} ions, as a result, M^{3+} and Ln^{3+} ions alternate regularly forming a simple chain. Other terminal or capping ligands, such as DMA (*N*,*N*-dimethylacetamide), DMF (*N*,*N*-dimethylformamide), betain, 2,2′-bipy (2,2′-bipyridine), attach to the lanthanide ions to furnish the coordination geometry. Interestingly, some of them exhibit unusual magnetic behavior, such as long range ordering and strong coercive force. Using CCl_3COO^- as a bridging ligand, another simple chain structure $Gd_2Cu(CCl_3COO)_8{\cdot}6H_2O$ can be obtained, in which the Cu^{2+} ion and a Gd_2 dimer locate alternately [78a]. The compound seems to behave as an antiferromagnet, but no quantitative analysis was done.

While employing 2,5-H_2pydc (pyridine-2,5-dicarboxylic acid) or 2,6-H_2pydc (pyridine-2,6-dicarboxylic acid) as ligands, chain Ln–TM compounds with different shapes can be obtained. For example, we obtained a zigzag chain structure formulated as $[\{Ln_2Cu_3(2,5\text{-pydc})_6(H_2O)_{12}\}{\cdot}4H_2O]_n$ (Ln = Er, Gd). This chain structure consists of two building blocks, cyclic $[Ln_2Cu_2(2,5\text{-pydc})_4(H_2O)_{12}]$ and $[Cu(2,5\text{-pydc})_2]^{2-}$, which connect to each other via Ln—O bonds. As a result, the two units are arranged alternately in the chain (Fig. 9). Eventually, some hydrogen bonds exist between the chains to form a 3D supramolecular structure [34c]. The χT value of the Gd^{3+} derivative increases slightly upon cooling and reaches a maximum at 40 K, revealing the ferromagnetic exchange between Gd^{3+}–Cu^{2+} pairs. The ferromagnetic interaction was further confirmed by the positive Weiss constant $\theta = 0.7857$ K. Cai et al. also reported a ∞ shaped compound $[\{Ln_4Cu_2(2,6\text{-pydc})_8(H_2O)_8\}{\cdot}18H_2O]_n$ (Ln = La, Pr) constructed from 2,6-H_2pydc. In this compound, 2,6-pydc ligands ligate to Cu^{2+} ions forming $[Cu(2,6\text{-pydc})_2]^{2-}$ units, which doubly bridge the Ln^{3+} ions into the ∞ shaped chain. For the La^{3+} derivative, a weak ferromagnetic Cu—Cu interaction can be observed [78b].

Using oxalate, opba or bpa as ligands, a ladder-type or tubular architecture can be obtained. Decurtins et al. reported a ladder-type architecture formulated as $[LnCr(ox)_3(H_2O)_4]_2{\cdot}12H_2O$ (Ln = La, Ce, Pr, Nd), in which both the sidepieces and the rungs of the ladder are formed by the oxalate bridges [78]. The χT values for the La, Ce, Pr, derivatives show a continuous decrease on lowering the temperature, which is attributed to the splitting of the electric levels on metal ions and/or the presence of weak exchange interaction. For the Nd derivative, the χT decreases first to reach a minimum at about 5 K and then increases. The authors claimed it as a ferrimagnet, but further magnetic studies should be carried out to support the conclusion.

A serials of 1D Ln–TM coordination polymers were also obtained using $[M(opba)]^{2-}$ (M = Cu, Ni, Zn) and $[Cu(pba)]^{2-}$ as building blocks. The former feature as ladder-type motifs, while the latter feature as either ladder-type or tube-type structures. For the ladder-type $\{Ln_2[M(opba)]_3\}{\cdot}S$ system (Ln = La–Lu, S for solvent molecules), the $[M(opba)]^{2-}$ moieties act both as the sidepieces and the rungs of the ladder to link the Ln^{3+} ions into a string [79] (Fig. 10a). The successful synthesis of the Zn^{2+} derivatives allows the authors to obtain independent information on the crystal-field and determine the nature of the exchange interactions of the Ln–TM pairs. For the Cu^{2+} derivatives, the Gd^{3+}–Cu^{2+}, Tb^{3+}–Cu^{2+} and Dy^{3+}–Cu^{2+} interactions are ferromagnetic, The Tm^{3+}–Cu^{2+} interaction might also be ferromagnetic but is uncertain. On the other hand, in all other cases, the Ln^{3+}–Cu^{2+} interaction is not ferromagnetic. For the Ni^{2+}–Ln^{3+} pairs, the interaction is ferromagnetic when Ln^{3+} is Gd^{3+}, Tb^{3+}, Dy^{3+}, and perhaps Ho^{3+}. However, when Ln^{3+} is Ce^{3+}, Pr^{3+}, Nd^{3+}, Er^{3+}, the interaction seems to be antiferromagnetic. Similar ladder-type compounds $\{Ln_2[Cu(pba)]_3\}{\cdot}S$ (Ln = Dy, Tb, Er) can also be obtained by slow diffusion in a H-shaped tube at room temperature, using equimolar aqueous solutions of $Na_2[Cu(pba)]{\cdot}6H_2O$ and Ln chloride [80]. In this system, the $[Cu(pba)]^{2-}$ units act as the sidepieces and the rungs of the ladder. For the Dy^{3+} derivative, the χT is constant until 10 K and then increases rapidly reaching 90 emu mol^{-1} K at 1.8 K, suggesting a ferromagnetic interaction. Ferromagnetic coupling is also observed for the Tb^{3+} and Er^{3+} derivatives. In addition, a beautiful tubular-like structure formulated as $Ln_2[Cu(pba)]_3{\cdot}20H_2O$ (Ln = Gd, Eu) can be synthesized with the same procedure described above but allowing slow crystallization at 70 °C [79] (Fig. 10b). There are two Ln^{3+} ions, three $[Cu(pba)]^{2-}$ moieties and several coordinated and lattice water molecules in the asymmetric unit of this structure. Two $[Cu(pba)]^{2-}$ moieties link the Ln^{3+} ions into chains, the third one connects four neighboring chains together to form a tube. The chains formed by $[Cu(pba)]^{2-}$ linked Ln^{3+} ions act as the wall of tube, while the third $[Cu(pba)]^{2-}$ is moiety trapped in the inner part of the tube. The Gd^{3+} derivative behaves as a 1D ferromagnet

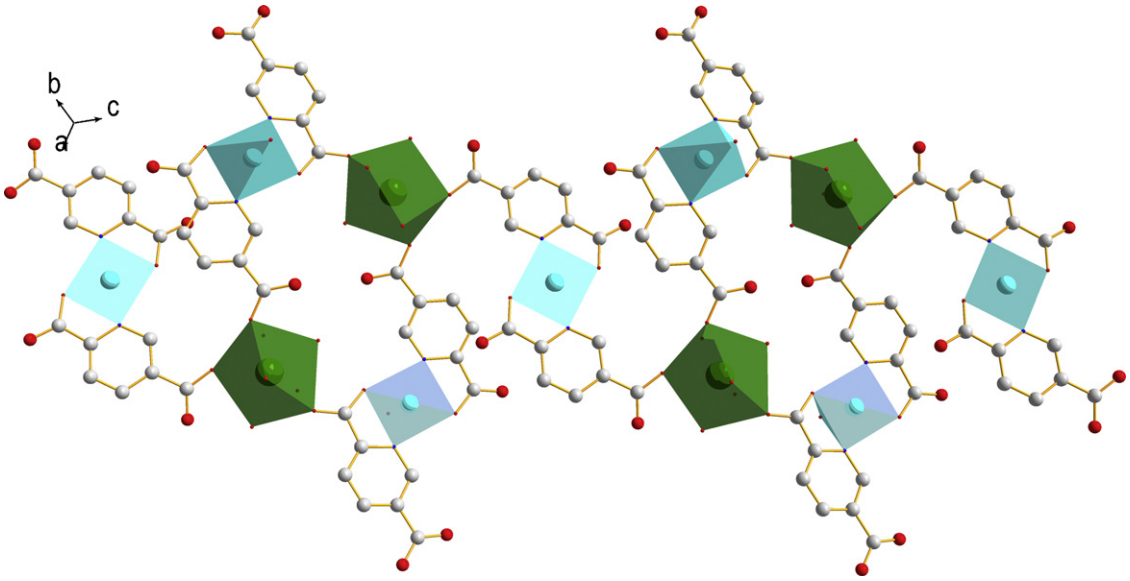

Fig. 9. The zigzag chain structure of $[\{Ln_2Cu_3(2,5\text{-pydc})_6(H_2O)_{12}\}\cdot 4H_2O]_n$ [34c].

with $\theta = 1.2$ K, while the χT value of the Eu^{3+} derivative surprisingly tends to be zero at low temperature.

3.4. Two-dimensional materials

2D Ln–TM structures are still rare in the literature. These reported Ln–TM compounds are generally constructed from either cyanide or multiple N- and O-donor ligands such as pyridine carboxylic acids.

3.4.1. Cyanide bridged layer structures

Initially, the magnetism of the cyano-bridged Ln–TM hybrid Prussian Blue coordination polymers was rarely investigated. Known cyano-bridged Ln–TM complexes such as dinuclear, trinuclear, tetranuclear, and one-dimensional chains do not seem exciting, since the coupling between the lanthanide and transition metals is very weak, because of the effective shielding of the 4f electrons by the outer-shell electrons. However, the 3D polymer $[SmFe(CN)_6]\cdot 4H_2O$, with strong anisotropic coercive field, exhibits long-range ferrimagnetic ordering below 3.5 K, and the similar polymer $[TbCr(CN)_6]\cdot 4H_2O$ has a high Curie temperature ($T_C = 11.7$ K). Encouraged by this exciting result, Gao et al. started their research interest on high dimensional cyano-bridged Ln–TM hybrid and obtained a series of compounds exhibiting interesting magnetic behavior.

Their interests are focused on 3d–4f compounds which are generally synthesized by slow diffusion or evaporation and using $[M(CN)_6]^{3-}$ (M = Fe, Co, Cr) which can be viewed as analogous to the metalloligand as precursor mentioned above. Their structures are various containing brick wall-like (6, 3) layer and unusual sheet structure with mixed nodes.

For instance, slow diffusion of $K_3[Cr(CN)_6]$, $Ln(NO_3)\cdot 6H_2O$ and DMF in a 1:1:2 molar ration in aqueous solution, generate a brick wall-like structure formulated as $[Ln(DMF)_2(H_2O)_3Cr(CN)_6]\cdot H_2O$ (Ln = Sm, Gd) [81]. In this compound, each $[Cr(CN)_6]^{3-}$ unit uses three cyanide groups to connect with three $[Ln(DMF)_2(H_2O)_3]^{3+}$ units. Each $[Ln(DMF)_2(H_2O)_3]^{3+}$ unit, in turn, connects to three $[Cr(CN)_6]^{3-}$ units, generating a flat brick wall-like layer. In topology view, both of the units define identical 3-connected nodes and the layer can be symbolized as a uniform (6, 3) net. For the Sm^{3+} derivative, due to the presence of the orbital contribution in the Sm^{3+} ground state, the observed decrease of χT upon cooling should be attributed to the superposition of thermal depopulation of the excited state of single Sm^{3+} ion and/or the antiferromagnetic Sm-Cr magnetic interaction. Although the nature of the magnetic interaction is unclear, long range magnetic order was observed confirmed by a magnetic phase transition below 4.2 K and a coercive field of 100 Oe at 1.85 K. For the Gd^{3+} derivative, the χT decreases smoothly with decreasing temperature, reaching a minimum at 100 K. With a further decrease in temperature, χT increases sharply reaching a maximum at 4.0 K and then decreases again, indicating ferrimagnetic behavior. Intralayer ferromagnetic interaction deriving from the uncompensated spins and long-range antiferromagnetic ordering due to the interlayer antiferromagnetic coupling were confirmed by further magnetic properties measurements. Furthermore, the "double-S" shape of its M–H curve suggests metamagnetism, which switches from an antiferromagnetic ground state to a ferrimagnetic-like state. Using

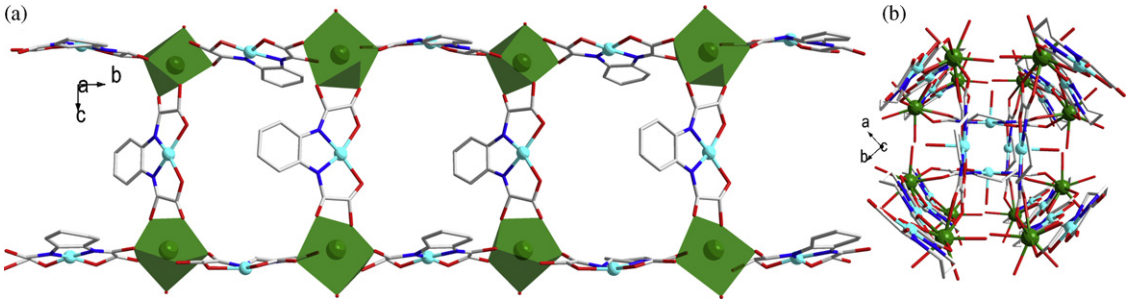

Fig. 10. (a) The ladder-type structure of $\{Ln_2[M(opba)]_3\}\cdot S$ [79a]; (b) the tube structure of $\{Ln_2[Cu(pba)]_3\}\cdot S$ [79c].

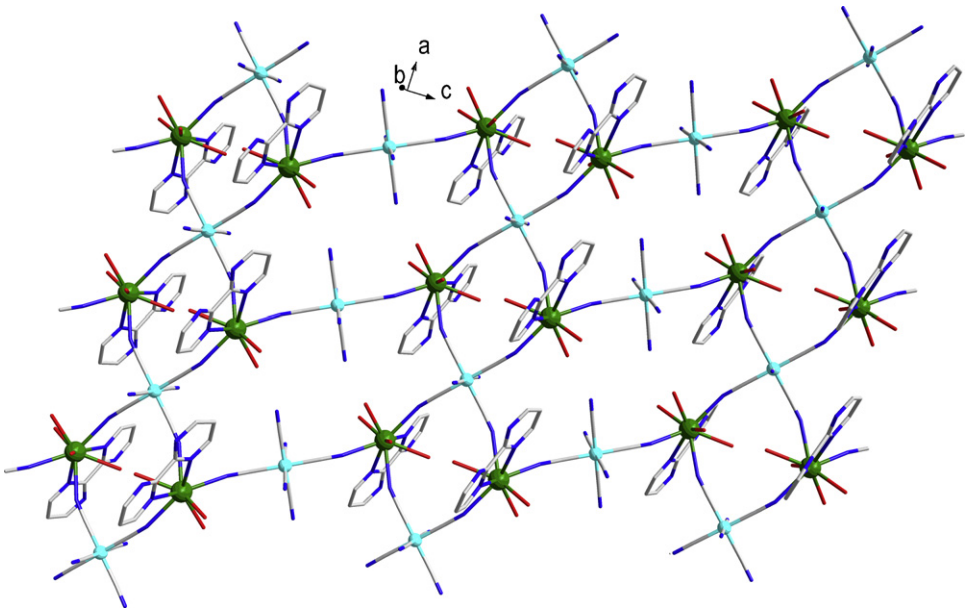

Fig. 11. The unusual layer structure of $[NdM(bpym)(H_2O)_4(CN)_6]\cdot 3H_2O$ with mixed nodes [82].

capping ligand bpym instead of terminal ligand DMF, a unique 2D structure formulated as $[NdM(bpym)(H_2O)_4(CN)_6]\cdot 3H_2O$ (M = Fe, Co) was synthesized (bpym = 2,2′-bipyrimidine) (Fig. 11) [82]. In the asymmetric unit of the structure, there are two crystallographically unequal M atoms and one Nd^{3+} ion. Both the M^{3+} ions are six coordinate via six CN groups with octahedral geometry. The Nd^{3+} ion is eight coordinate via four water molecules, four nitrogen atoms from two CN groups, and one bypm ligand. One $[M(CN)_6]^{3-}$ center uses four CN^- groups in the same plane to connect to Nd^{3+} ions, resulting in a double strand chain comprising 12-membered rhombus subunits $M_2Nd_2(CN)_4$; the other $[M(CN)_6]^{3-}$ center uses two *trans* CN^- groups to link neighboring chains, leading to an unusual 2D sheet structure with alternating fused rows of rhombus-like $M_2Nd_2(CN)_4$ rings and six sided $M_4Nd_4(CN)_8$ rings. Treating the Nd^{3+} ions and the first type of $[M(CN)_6]^{3-}$ centers as nodes, the 2D layer can be viewed as a net with (3, 4)-connected mixed nodes. In this system, for the Co^{3+} derivative, the χT decreases continuously with decreasing the temperature; while for the Fe^{3+} derivative, the χT decreases first reaching a minimum at 10 K and then increases rapidly. The comparison of the magnetic properties of these two derivatives suggests that the coupling between Fe^{3+} and Nd^{3+} ions is ferromagnetic. Unexpectedly, the Co^{3+} derivative showed a puzzling behavior of the ac susceptibility measured in the presence of an applied field of 2 kOe. While measured at zero field, it showed normal paramagnetic behavior. This field dependent relaxation analogous to that observed in spin glasses or superparamagnets was tentatively attributed to spin glass behavior generated by spin frustration.

In addition to the 3d–4f hybrid Prussian Blue coordination polymers above, some other groups reported several examples of 2D 4d–4f and 5d–4f cyano-bridged coordination polymers which are synthesized by using the $[Ru^{II}(CN)_6]^{4-}$ as well as $[W(CN)_8]^{3-}$ as building blocks. The structures of these compounds are diverse, varying from brick wall layer to highly ordered (4, 4) sheet. Ward and coworkers reported a 2D compound $[Ru(phen)(CN)_4]_3[Gd(phen)(H_2O)_3]_2\cdot 6H_2O$ in which the $[Ru(phen)(CN)_4]^{2-}$ units link the Gd^{3+} ions into 2D brick wall layer structure (phen = 1,10-phenanthroline) [83b]. Notably, Hashimoto and coworkers obtained a 2D Sm^{3+}–W^{5+} complex $Sm(H_2O)_5[W(CN)_8]$ with a highly ordered (4, 4) layer structure [83c]. For this compound, when the sample was slowly cooled from 300 to 10 K at a cooling rate of −1 K min^{-1}, the *M* vs *T* curve showed antiferromagnetism with a Néel temperature (T_N) of 3.0 K. Conversely, when the sample was placed directly into a sample chamber at T = 10 K, ferromagnetism with a T_C of 2.8 K was observed. On the basis of calculations considering interlayer superexchange interactions and interlayer dipole-dipole interactions, the authors ascribed the observed cooling-rate dependent ferromagnetism to be understood by a change of the interlayer superexchange interactions.

In addition, reaction of $Tb(NO_3)_3\cdot 6H_2O$ and $Ph_4P[Ru(acac)_2(CN)_2]$ gave a different wavy (4, 4) layer structure $Ph_4P\{Ln(NO_3)_2[Ru(acac)_2(CN)_2]_2\}$ (Ln = Tb, Dy, Er, Gd) [83a]. In this compound, each Ln^{3+} ion is eight coordinate through four oxygen atoms from two nitrate ions and four nitrogen atoms of cyano groups of four $[Ru(acac)_2(CN)_2]^-$ ions. As a result, the $[Ru(acac)_2(CN)_2]^-$ ions act as linkers to bridge the Ln^{3+} ions into a wavy (4, 4) layer. However, the magnetic coupling between the Ln^{3+} and Ru^{3+} ions via the cyano bridges is negligibly weak.

3.4.2. Two-dimensional materials based on multiple N-/O-donor ligands

Although multidentate ligands containing mixed N- and O-donor atoms are considered as good candidates to construct Ln–TM hybrid materials, 2D Ln–TM compounds based on them are still limited. Except for the compounds mentioned above based on Ln–TM clusters or metalloligands, there are several others mainly constructed from pyridine carboxylic acid ligands. Their structures are diverse containing sandwich structure, 2-fold penetrating corrugated brick wall frameworks, as well as a typical honeycomb structure with (6, 3) net.

As far as we know, there is no 2D Ln–TM compound constructed from pyridine monocarboxylic acids or pyridine tricarboxylic acids, while several compounds with different topologies are constructed from pyridine dicarboxylic acids. Unfortunately, due to the large distances between paramagnetic centers, the magnetic interactions are weak.

Employing pyradine-2,4-dicarboxylic acid (2,4-H_2pydc), we synthesized a two-fold interpenetration corrugated brick wall layer structure with (6,3) topology $[LnCo(pydc)_3(H_2O)_3]_n\cdot xH_2O$ (Ln = Eu, Yb) [74f]. The asymmetric unit for this compound contains one $[Co(2,4\text{-}pydc)_3]^{3-}$ anion and one Eu^{3+} ion. Each $[Co(2,4\text{-}pydc)_3]^{3-}$ unit connects to three Eu^{3+} ions and in turn each Eu^{3+} ion connects to three $[Co(2,4\text{-}pydc)_3]^{3-}$ metalloligands, leading to a corrugated

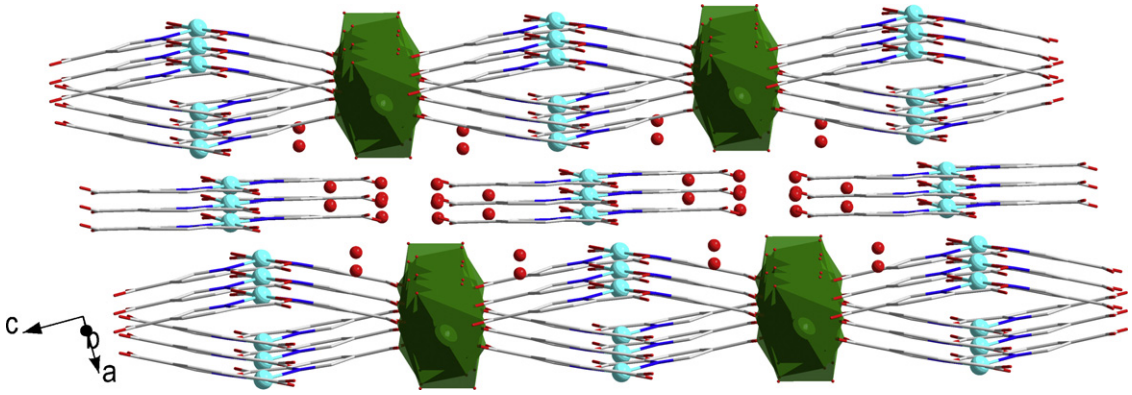

Fig. 12. The sandwich structure of $[\{Gd_2Cu_2(2,5\text{-pydc})_4(H_2O)_8\}\cdot Cu(pydc)_2\cdot 12H_2O]_n$ [34b].

brick wall structure with (6,3) topology. In addition, two such sheets interpenetrate together forming a 2-fold interpenetrating layer structure with solvent-filled channels. The χT values for both compounds in this system show a continuous decrease with decreasing temperature suggesting possible weak antiferromagnetic coupling between Ln^{3+} ions. Using 2,5-H_2pydc, we obtained two compounds with formulae $[Gd_2Ag_2(pydc)_4(H_2O)_4]_n$ and $[\{Gd_2Cu_2(2,5\text{-pydc})_4(H_2O)_8\}\cdot Cu(pydc)_2\cdot 12H_2O]_n$ [74a,34b]. For the first structure, the Gd^{3+} is coordinated by two nitrogen atoms and six oxygen atoms of which four arise from different 2,5-pydc ligands. The Ag^+ is coordinated by two oxygen atoms from different 2,5-pydc ligands in a nearly linear fashion. The Gd^{3+} ions are first linked forming double chains which are further connected together to generate the final 2D structure through Ag—O bonds. The second compound has a sandwich structure which consists of an infinite layer like $[Gd_2Cu_2(2,5\text{-pydc})_4(H_2O)_8]$ cation and discrete $[Cu(2,5\text{-pydc})_2]$ anion units and water molecules (Fig. 12). As to the $[Cu(2,5\text{-pydc})_2]$ anion, the Cu^{2+} ion is chelated by two

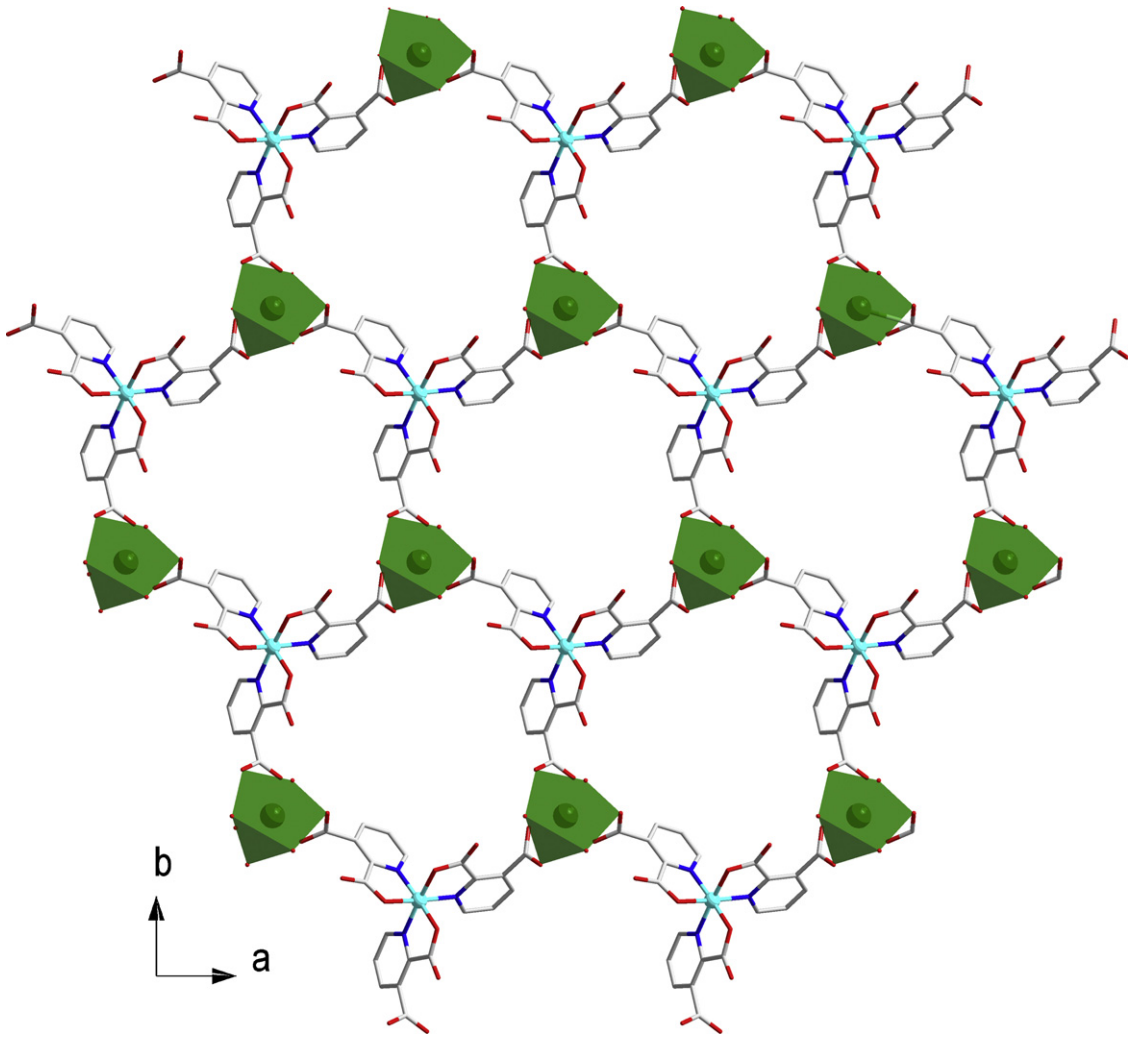

Fig. 13. The honeycomb structure of $[GdCo(2,3\text{-pydc})_3(H_2O)_3]_n$ [84a].

2,5-pydc ligands through nitrogen and oxygen atoms from 2-carboxylate groups in an exactly square planar geometry. The $[Gd_2Cu_2(2,5\text{-pydc})_4(H_2O)_8]$ cation layer can be viewed as Gd^{3+}-linkers connected $[Cu(2,5\text{-pydc})_2]^{2-}$ building blocks. As a result, carboxylate-bridged Gd^{3+} chains exist in the layer-like cation. The discrete $[Cu(pydc)_2]^{2-}$ anions are inserted between two cation layers, generating the final sandwich like structure.

While using 2,3-H_2pydc (pyridine-2,3-dicarboxylic acid) or 3,5-H_2pydc (pyridine-3,5-dicarboxylic acid), porous honeycomb structure or herringbone structure with (6, 3) net was obtained, respectively. Hydrothermal reaction of $Co(Ac)_2{\cdot}4H_2O$, $Gd(NO_3)_3$ and 2,3-H_2pydc in aqueous solution at 140 °C generated the first honeycomb structure $[GdCo(2,3\text{-pydc})_3(H_2O)_3]_n$ (Fig. 13) [84a]. This compound contains $[Co(2,3\text{-pydc})_3]^{3-}$ anions which act as μ_3-bridges. Each $[Co(2,3\text{-pydc})_3]^{3-}$ unit uses its three 3-carboxylate groups of three 2,3-pydc moieties to connect to three nine coordinated Gd^{3+} ions. As a result, the Gd^{3+} ions are extended by $[Co(2,3\text{-pydc})_3]^{3-}$ anion forming a honeycomb sheet with large Gd_3Co_3 rings. Interestingly, on heating at 700 °C, this compound transforms into a perovskite oxide. The second herringbone structure $[\{Ln_2M_3(3,5\text{-pydc})_6(H_2O)_{22}\}{\cdot}20.5H_2O]_n$ (Ln = Sm, Eu, Gd; M = Co, Ni) was synthesized by slow diffusion [84b]. Distinct from the first structure, two 3,5-pydc ligands ligate to one M^{2+} ion to give rise to a $[M(3,5\text{-pydc})_2]^{2-}$ unit which acts as μ_2-linker in the layer structure. Each Ln^{3+} ion connects to three adjacent ones through $[M(3,5\text{-pydc})_2]^{2-}$ unit resulting in the herringbone structure with Gd_6Co_6 rings. Remarkably, a novel water aggregate, comprised of alternate octameric water cubes and $(H_2O)_{20}$-cluster units, was encapsulated within the crystal lattice of the metal–organic networks.

In addition, honeycomb Ln–TM structures were also synthesized by using H_2pzdc (pyrazine dicarboxylic acid) or H_2opba as ligands. For example, Zheng and coworkers reported a honeycomb coordination polymer $[LnCu(2,6\text{-pzdc})_3]{\cdot}[Ln(H_2O)_9]_{0.5}{\cdot}[(H_2O)_7H^+]_{0.5}$ (Ln = La, Eu, Gd) with supramolecular 1D channels, in which lanthanide hydrate cations and lattice water molecules are located [85a]. Using $Na_2[Cu(opba)]$ as precursor, another honeycomb structure formulated as $\{Nd_2[Cu(opba)_{0.5}(ox)]_3{\cdot}9DMF\}{\cdot}4.5DMF$ was obtained, in which the oxalate (ox) was afforded by partial hydrolysis of the $Nd_2[Cu(opba)]$ during the reaction [85b]. In the hexagonal structure, the Nd^{3+} ions locate at the conjunctions of the hexagons and the $Cu(opba)^{2-}$ acts as the sides. Upon cooling, the χT curve decreases continuously and tends to go to zero down to 0 K. It is unusual for a 2D magnetic compound with an odd number of unpaired electrons. This phenomenon may be due to the accidental cancellation at low temperature of the moment associated with the two Nd^{3+} ions and three Cu^{2+} ions.

3.5. Three-dimensional materials

3.5.1. Materials based on single ligand

About 30 years ago, cyanide bridged Prussian blue like Ln–TM molecular magnets were obtained. For example, isostructural 3D Prussian blue like compounds $[SmFe(CN)_6]{\cdot}4H_2O$ and $[TbCr(CN)_6]{\cdot}4H_2O$ exhibit important magnetic properties. In fact, the former orders as a ferrimagnet at about 3.5 K with a strong coercive field, while the latter has high critical temperature (T_C = 11.7 K) [86]. Until now, various ligands have been largely employed to construct 3D Ln–TM coordination polymers. Among these, H_2oda (oxydiacetic acid) was used to construct 3D Ln–TM structure with hexagonal or cubic topologies [69], benzenecarboxylic acids were used to synthesize Ln–Cu metal–organic frameworks based on rod-shaped and (6,3)-sheet [6], while pyridine carboxylic ligands were more widely employed due to their abundant coordination modes to synthesize 3D coordination polymers with diverse topologies and magnetic properties [74]. Furthermore, the cooperativity of different ligands was introduced by Yang and coworkers to construct 3D Ln–TM coordination polymers based on lanthanide or transitional metal clusters [73b].

Oxydiacetic acid (H_2oda), having five potential oxygen-donor atoms, has been satisfactorily used in the assembling of lanthanide and copper ions in the series of 3D complexes with formula $[\{Cu_3Ln_2(oda)_6(H_2O)_6\}{\cdot}12H_2O]_n$ (Ln = Y, Gd, Eu, Nd, Pr, Dr, Er) (Fig. 14a) [87]. Reaction of Ln_2O_3, CuO and H_2oda in aqueous solution gave the 3D compounds. The complexes in this system crystallize in the high *P*6/*mcc* space group. The lanthanide constriction seems to influence the crystallizing process, the homologous polymers for the two larger La and Ce ions crystallize in the hexagonal system, space group $P\bar{6}2c$ [88]. Each four coordinate Cu^{2+} ion connects to four nine coordinate Ln^{3+} ions by two oda^{2-} ligands defining a 4-connecte node. Each Ln^{3+} ion connects to six Cu^{2+} ions via three oda^{2-} ligands defining a 6-connecte node. As a result, a porous framework with solvent filled channels along *c* axis is formed. From a topological view, this framework can be simplified as a (4,6) connected net with $(4^4{\cdot}6^2)(4^9{\cdot}6^6)$ Schläfli symbol (Fig. 14b). For the Y^{3+}, Dy^{3+}, Ho^{3+} and Gd^{3+} derivatives, upon cooling, their χT values remain constant at first and then decrease rapidly, while for the Eu^{3+}, Nd^{3+}, Er^{3+} and Pr^{3+} derivatives,

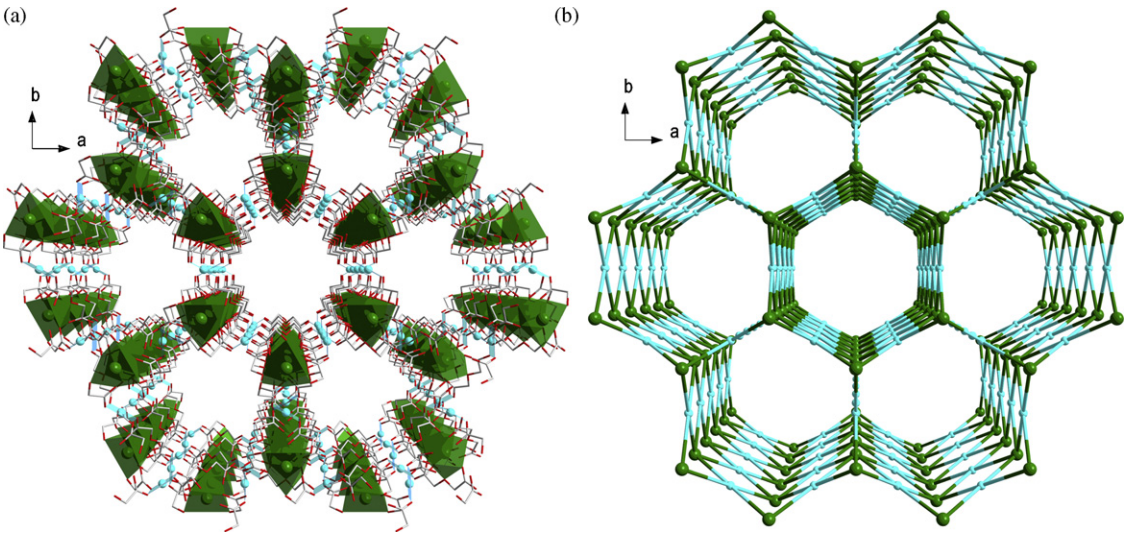

Fig. 14. (a) The 3D hexagonal structure of $[\{Cu_3Ln_2(oda)_6(H_2O)_6\}{\cdot}12H_2O]_n$; (b) topology view of its (4, 6)-connected net [87].

a monotonical decrease of χT was observed. Therefore, all these compounds behave as weak antiferromagnets. Interestingly, using Mn^{2+} ions with octahedral coordination geometry instead of Cu^{2+} ions with square geometry, a cubic network was obtained [69]. Hydrothermal reaction of $Gd(NO_3)_3{\cdot}5H_2O$, $MnSO_4{\cdot}H_2O$ and H_2oda generated a different 3D porous framework with formula $[\{Mn(H_2O)_6\}\{MnGd(oda)_3\}_2]{\cdot}6H_2O$. By contrast, the Mn^{2+} ions in the complex are coordinated by six oxygen atoms from three oda ligands with octahedron geometry. As the result, each Mn^{2+} ion connects to six Gd^{3+} ions, each Gd^{3+} ion in turn links to six Mn^{2+} ions, giving rise to a porous framework with NaCl net. Isolated $Mn(H_2O)_6{}^{2+}$ ions and lattice water molecules are filled in the channels. With decrease of temperature, χT remains constant to about 10 K and then increases rapidly, indicating only ferromagnetic interaction between the Gd^{3+} and Mn^{2+} ions with $J = 0.24\,cm^{-1}$.

Due to the rigidity and abundant coordination modes to metal ions, benzenecarboxylic acids show their great ability to construct coordination polymers with various topologies [89]. However, research in the Ln–TM area based upon benzenecarboxylic acids still remains to be explored. The carboxylate O atoms prefer to link to lanthanide ions than transition metal ions, thus it is difficult to introduce transition metal ions into the final products without the assistance of N donor ligands in the reaction system.

There appears to be only one Ln–TM compound, in the CCDC database, constructed solely from isophthalic acid (H_2ip). Reaction of Ln_2O_3, $Cu(NO_3)_2$ and H_2ip under hydrothermal condition generated the compound $[Cu_3Ln_2(ip)]$ (Ln = Eu, Gd) [6]. In the metal carboxylate substructure, the metal ions are bridged into a 2D hexagonal network, with Eu centers acting as nodes, and Cu^{2+} ions lying midway along an edge. The ip^{2-} ligands pillar the layers into an overall 3D network with two different cavities. Actually, when the required N donor ligands were introduced, a variety of Ln–TM coordination polymers were obtained. In this system, the N donor ligands either act as capping ligands coordinated to TM ions or cooperate with benzenecarboxylic acids to connect the metal ions into a 3D network.

Using 2,2′-bipyridine (2,2′-bipy) as ancillary ligands, our group and others obtained several 3D Ln–TM compounds based on isophthalic acid (H_2ip) [6,74d]. Reaction of Gd_2O_3, $Cu(NO_3)_2{\cdot}3H_2O$, H_2ip and 2,2′-bipy in 1:2:1:2 molar ration generated $[\{[Gd_4(ip)_7(H_2O)_2][Cu(2,2'\text{-bipy})_2]_2\}_n]$ (Fig. 15a). During the reaction, the Cu^{2+} was reduced to Cu^{+} by excess 2,2′-bpy. This compound has charged cages containing two encapsulated $[Cu(bipy)_2]^+$ ions. The Gd^{3+} ions are first linked by two oxygen atoms to form a Gd_2O_2 building unit, then eight Gd_2O_2 units are linked together by ip^{2-} ligands to generate a large charged cage, in which two $[Cu(bipy)_2]^+$ ions with a distorted tetrahedral geometry are trapped as charge-compensating guests. Reducing the amount of 2,2′-bipy added, another compound with formula $[Gd_3Cu(ip)_5(Hip)(2,2'\text{-bipy})]_n{\cdot}H_2O$ was synthesized (Fig. 15b). The Gd^{3+} ions are also linked into a 3D network with cavities by ip ligands, while the $[Cu(bipy)]^{2+}$ ions bind the inner backbone of the cavity forming the 3D structure. From the view of topology, the 3D structure can be viewed as α-Po net treating rod-shaped Gd_6Cu_2 subunits as nodes and ip ligands as linkers. For these two compounds, the magnetic interactions between metal ions are very weak. For the first, the χT value decreases slightly to 12 K, and then dramatically decreases. The spin-coupled dimer model ($H = -JS{\cdot}S$) was applied to perform a quantitative analysis leading to $g = 2.08$ and $J = -0.09\,cm^{-1}$. For $[Gd_3Cu(ip)_5(Hip)(bipy)]_n{\cdot}H_2O$, the χT plot is almost constant from 300 to 50 K, increases as temperature is lowered, reaching a maximum value around 10 K, and then decreases again. Simulating the result with a linear octanuclear model indicates that the Gd^{3+}–Gd^{3+} interaction is weak antiferromagnetic and the Gd^{3+}–Cu^{2+} interaction is ferromagnetic. Recently, Zheng et al. reported a similar Ln–TM compound $[Ln_2Cu_3(ip)_6(2,2'\text{-bipy})_2]{\cdot}5(H_2O)_5$ (Ln = Yb, Gd, Tb) (Fig. 15c). The ip ligands first link the Ln^{3+} ions into a (6, 3) layer. Different from the two compounds above, two crystallographic Cu^{2+}, one connecting the (6, 3) layers into a 3D framework with cavities, the other chelated by 2,2′-bpy attaching the 3D framework occupying the cavities. The 3D framework also can be considered as α-Po net, if rod-shaped Ln_3Cu_2 motifs are treated as nodes and ip

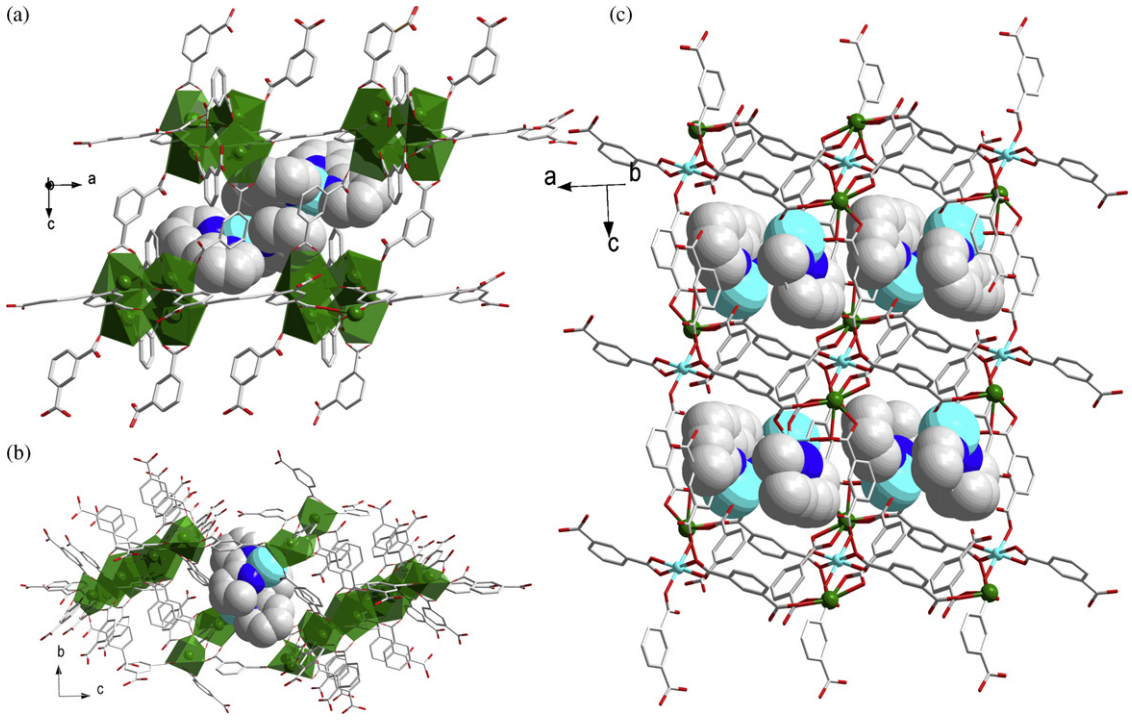

Fig. 15. (a) The structure of $[\{[Gd_4(ip)_7(H_2O)_2][Cu(2,2'\text{-bipy})_2]_2\}_n]$ [74d]; (b) the structure of $[Gd_3Cu(ip)_5(Hip)(2,2'\text{-bipy})]_n{\cdot}H_2O$ [74d]; (c) the structure of $[Ln_2Cu_3(ip)_6(2,2'\text{-bipy})_2]{\cdot}5(H_2O)_5$ [6].

ligands as linkers. Magnetic studies for the compounds in this system reveal antiferromagnetic-like behavior, but the nature remains to be clarified since it may be related to the progressive thermal depopulation of the Ln^{3+} Stark components.

Pyrazine carboxylic acids being ligands containing multiple *N*- and *O*-donors should be good candidates to construct extended Ln–TM coordination polymers. Surprisingly, only two Ln–TM compounds based on this kind of ligand were reported. One is a 2D (6, 3) layer structure described above, the other one is a 3D coordination polymer with formula $[Ln_2Zn(2,3\text{-pzdc})_4(H_2O)_6{\cdot}2H_2O]_n$ (2,3-H_2pzdc = pyrazine 2,3-dicarboxylic acid) (Ln = Gd, Nd, Sm) obtained by us [74c]. Two 2,3-$pzdc^{2-}$ anions exist in the 3D structure: one links the Zn^{2+} ions into a tape, the other links the Ln^{3+} ions into a wave-like layer structure. The pzdc ligands belonging to the Zn^{2+} tapes further ligates to Ln^{3+} ions using its one of the carboxylate *O* atoms forming the final 3D brick-like structure.

Compared to the silence of Ln–TM coordination polymers based on pyrazine carboxylic acids, the research on pyridine carboxylic acids is very active. A variety of compounds ranging from 1D to 3D structures were obtained. According to the number of carboxylic groups in the ligands, the pyridine carboxylic acids can be divided into three types: pyridine monocarboxylic acid, pyridine dicarboxylic acid and pyridine tricarboxylic acid, as illustrated in Scheme 4.

The simplest is pyridine monocarboxylic acid which contains picolinic acid (pic), nicotinic acid (na) and isonicotinic acid (ina). Reports on 3D Ln–TM compounds constructed from picolinic acid or nicotinic acid are still very limited. For picolinic acid, no 3D Ln–TM coordination polymers were reported. For nicotinic acid, Gu and Xue present a 3D Nd–Cu framework incorporating discrete cubane Cu_4 clusters covalently bonded to lanthanide centers [90]. Because isonicotinic acid (ina) has oxygen and nitrogen donors on opposite sides, 3D Ln–Cu coordination polymers constructed from it have been widely explored. They present diverse structural features: isonicotinic acid linked clusters, isonicotinic acid linked wheels and pillared Ln–TM frameworks.

Yang and coworkers obtained a 3D coordination framework with formula $[Ln_{14}(\mu_6\text{-O})(\mu_3\text{-OH})_{20}(ina)_{22}Cu_6Cl_4(H_2O)_8]{\cdot}6H_2O$ (Ln = Y, Gd, Dy) based on linkage of nanosized lanthanide clusters and copper centers using isonicotinic acid [91]. The Ln^{3+} ions are linked together through hydrophilic hydroxo and oxo bridges to give a novel tetradecanuclear $[Gd_{14}(\mu_6\text{-O})(\mu_3\text{-OH})_{20}]^{20+}$ cluster pyramids, the Ln_{14} core consists of one octahedral $[Gd_6(\mu_6\text{-O})(\mu_3\text{-OH})_8]^{8+}$ unit that shares two opposing Ln apexes with two novel $[Gd_5(\mu_3\text{-OH})_6]^{4+}$ trigonal bipyramids (Fig. 16a). The Cu^+ centers either are bonded to four ina ligands or are bridged by Cl^- to form a Cu_2Cl_2 dimer. The ina ligands connect the Ln_{14} core and the Cu^+ centers into the overall 3D network with 1D channels filled by water molecules and terminal ina ligands. For the Gd and Dy derivatives, possible antiferromagnetic interactions exist between the Ln^{3+} ions. Another 3D Ln–TM coordination polymer based on isonicotinic acid linked clusters was reported by Zheng and coworkers [92]. Reaction of Gd_2O_3, $CuCl_2$, Hina, $(NH_4)HCOO$ and $HClO_4$ generated $[Gd_2Cu^{II}{}_2Cu^{I}{}_5(ina)_{10}(\mu_2\text{-Cl})(\mu_2\text{-OH}_2)_2(\mu_3\text{-OH})_2]{\cdot}(ClO_4)_2$, which is a self-penetrating net based on an unusual α-Po net with double edges constructed from a 12-connected Gd_2Cu_2 core. Two Gd^{3+} ions and two Cu centers are bridged together via two $\mu_2\text{-O}_{carboxylate}$ atoms, two μ_2-OH_2 molecules and two μ_3-OH^- ions to give rise to a planar tetramer cluster. Each tetramer core connects to 12 others through four ina^- anions and four linear $Cu(ina)_2$ fragments, as

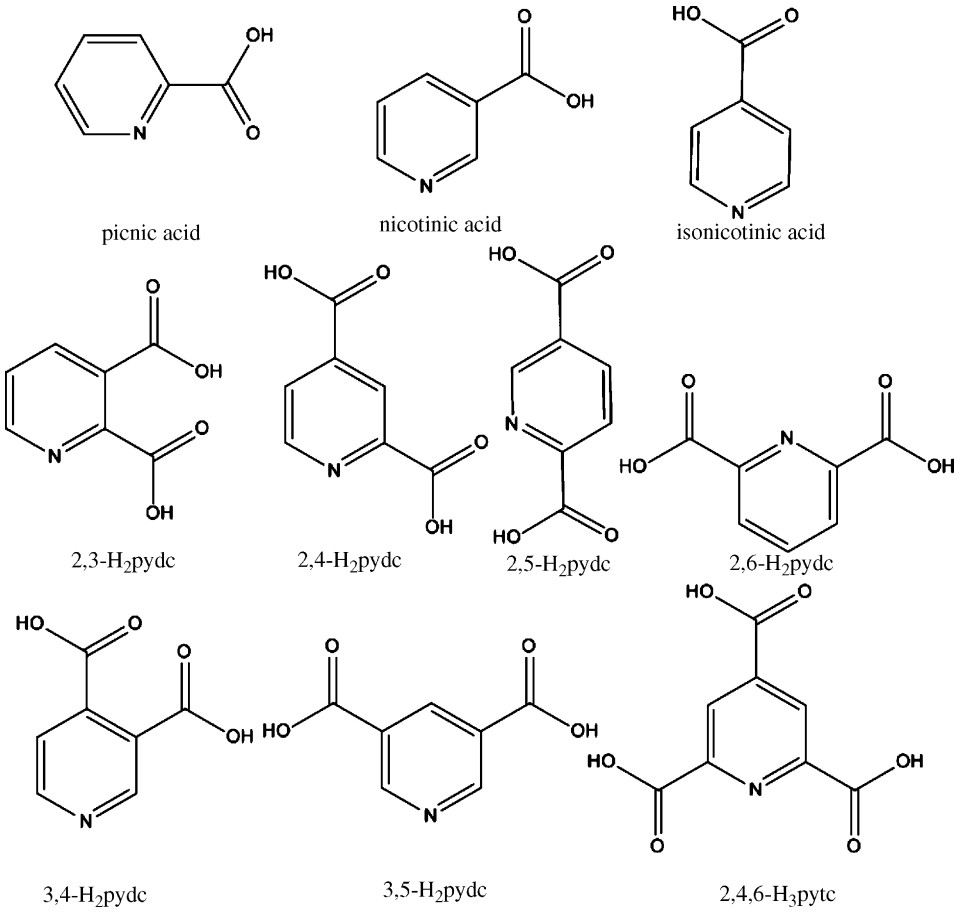

Scheme 4. All the pyridine carboxylic acid.

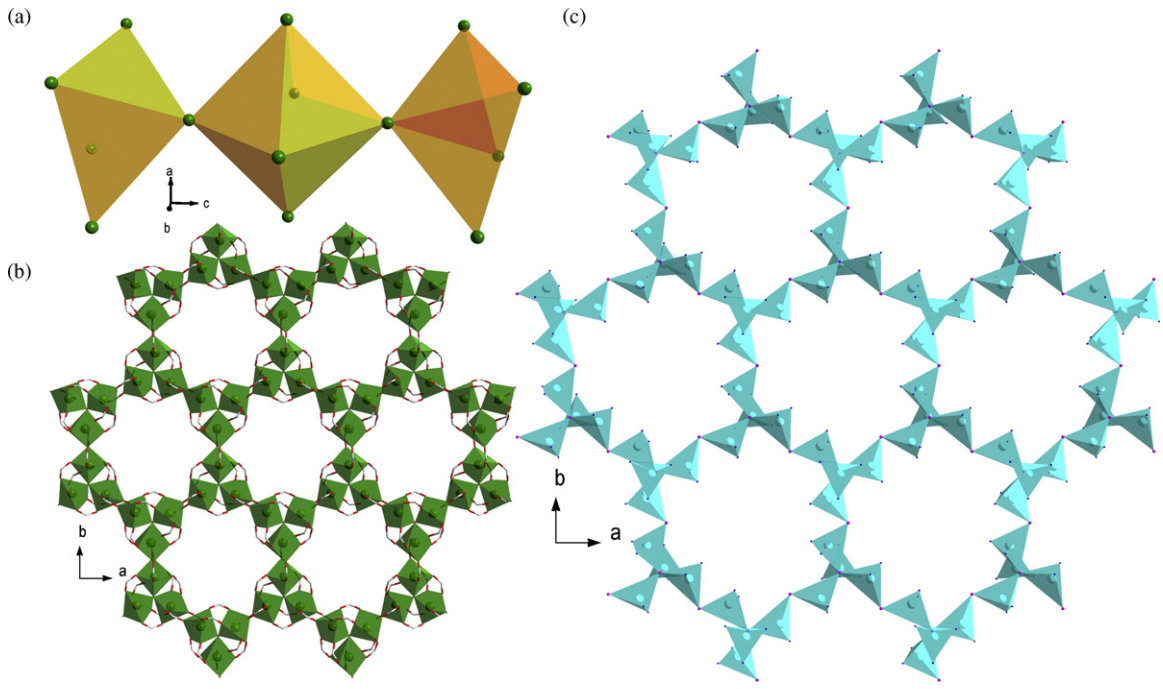

Fig. 16. (a) The Ln_{14} core in $[Ln_{14}(\mu_6\text{-}O)(\mu_3\text{-}OH)_{20}(ina)_{22}Cu_6Cl_4(H_2O)_8]\cdot 6H_2O$ [91]; (b and c) the layer of $\{Er_{18}\}$ wheels (b) and $\{Cu_{24}\}$ wheels in $[Ln_6(\mu_3\text{-}O)_2](ina)_{18}[Cu_8(\mu_4\text{-}I)_2(\mu_2\text{-}I)_3]H_2O$ (c) [73a].

well as two H-shaped $Cu_2(\mu_2\text{-}Cl)(ina)_4$, resulting in the final self-penetrating net. Upon cooling, its χT increases slightly to reach a maximum at around 50 K, and then sharply decrease because of the dipolar–dipolar and/or antiferromagnetic interaction. Applying Curie–Weiss law to analyze the result, a plus θ value ($\theta = 0.9$) was obtained, indicating weak ferromagnetic behavior. Furthermore, at 2 K, the M values rapidly increase at 0–15,000 Oe, confirming the ferromagnetic behavior. Although no suitable model was applied to simulate the experimental data, this compound possesses the potential function as a molecule-based magnetic material.

Another important structural feature of 3D Ln–TM coordination polymer constructed from isonicotinic acid is isonicotinic acid linked wheels. Yang and coworkers reported a series of Ln–Cu cluster complexes with formula $[Ln_6(\mu_3\text{-}O)_2](ina)_{18}[Cu_8(\mu_4\text{-}I)_2(\mu_2\text{-}I)_3]H_2O$ (Ln = Y, Nd, Dy, Gd, Sm, Eu, Tb) [73a]. In this system, two unusual trinuclear $[Ln_3(\mu_3\text{-}O)]$ and tetranuclear $[Cu_4(\mu_4\text{-}I)]$ cores are successfully assembled into two different nanosized wheels $[Ln_{18}(\mu_3\text{-}O)_6(CO_2)_{48}]^{6-}$, $\{Ln_{18}\}$ (Fig. 16b), and $[Cu_{24}(\mu_4\text{-}I)_6(\mu_2\text{-}I)_3]^{6+}$, $\{Cu_{24}\}$ (Fig. 16c). The wheels are further extended into 2D $\{Ln_{18}\}$ and $\{Cu_{24}\}$ layers, which are pillared by ina ligands to form 3D sandwich-like frameworks. Except for the Gd derivative, it is difficult to determine the magnetic nature of the compounds due to the spin orbital couple of lanthanide ions and the complicated topology. For the Gd derivative, the intratrinuclear interaction was very weak antiferromagnetic with $J = -0.031\ cm^{-1}$. Interestingly, it exhibits a field induced frequency-dependent magnetic behavior which may be explained by the magnetic behavior of an isolated ion; the lifting of the Kramer degeneracy by the applied magnetic field is responsible for this magnetic behavior. Xue and coworkers also reported a Ln–Cu compound with formula $Ln_4(\mu_3\text{-}OH)_2Cu_6I_5(ina)_8(OAc)_3$ (Ln = Nd, Pr) constructed from isonicotinic acid linked wheels [93a]. Three crystallographic unique Ln^{3+} ions are linked by one μ_3-OH to generate a $[Ln_3(\mu_3\text{-}OH)_2]^{7+}$ core, and then the $[Ln_3(\mu_3\text{-}OH)_2]^{7+}$ core links another one to form a chair like $[Ln(\mu_3\text{-}OH)_4]^{14+}$ core. The $\{Ln_6\}$ cores and another $\{Ln_2\}$ core are connected alternately to form a nanosized $\{Ln_{16}\}$ wheel. The $\{Ln_{16}\}$ wheels then are linked to surrounding wheels to form a layer of $\{Ln_{16}\}$ wheels. On the other hand, the Cu^+ ions are bridged into a chain of $\{Cu_6I_5\}$ clusters through Cu—I bonds. The ina ligands pillar the layers of $\{Ln_{16}\}$ wheels and the copper halide chains together form the 3D framework. Instead of isonicotinic acid linked wheels, a dimeric $[Ln_2(ina)_6]$ core linking $[Cu_8I_7]_n^{n+}$ layers was also reported in the literature [93b].

In addition, Zheng and coworkers reported a 3D Ln–Cu compound $Gd_3(ina)_{10}(\mu\text{-}OH_2)_6Cu_5(\mu_2\text{-}Cl)_4(H_2O)$ constructed from diverse pillared carboxylate-bridged lanthanide layers employing ina ligands [94]. The Gd^{3+} ions are bridged into 2D (4, 4) sheet by carboxylic groups from ina ligands. Three types of pillars: two different H-shaped pillars and (double acalixarene)-related pillars, pillared the (4, 4) sheets into the 3D framework. Upon lowering the temperature, the χT value increases steadily from 300 to 70 K and then decreases sharply. The increase of χT is typical of a ferromagnetic interaction between Gd^{3+} ions, which is further confirmed by its M–H curve. The decrease of χT at low temperature may be ascribed to antiferromagnetic and/or dipolar–dipolar interactions.

Pyridine dicarboxylic acids and pyridine tricarboxylic acids are also viewed as good candidates to construct 3D Ln–TM compounds. However, interest mostly focuses on 2,5-H_2pydc and 2,6-H_2pydc, although a few reports on 3D Ln–TM compounds constructed from other ligands can be found in the literature. The structures of the compounds in this system are diverse, containing 3D networks constructed from clusters, pillared layers, 3D porous framework, etc.

Using 2,5-H_2pydc, Yue and coworkers reported a 3D Ln–TM antiferromagnet with formula $[Gd_4Co^{II}Co^{III}(\mu_3\text{-}OH)_3(\mu_3\text{-}O)(2,5\text{-}pydc)_6(H_2O)_5]\cdot 8H_2O$ constructed from Gd_4 clusters and Co_2 subunits [95]. The Gd^{3+} ions are clustered together by μ_3-OH forming a tetrahedron, the Co^{2+} and Co^{3+} ions are bridged into a dinuclear subunit by carboxylate groups. Finally, the tetrahedral Gd_4 cluster connects to the Co_2 subunits by 2,5-pydc ligands forming a 3D framework with α-Po topology.

Several compounds constructed from pillared layers were obtained by us and other groups. Employing 2,4-H_2pydc as ligand, two 3D Ln–Cu coordination polymers were obtained with formula $[Gd_2Cu(2,4\text{-}pydc)_4(H_2O)_6]_n$ and $[Ln_2Cu_3(2,4\text{-}pydc)_6(H_2O)_6]_n$ (Ln = Sm, Er, Tb) [34,74e]. For $[Gd_2Cu(2,4\text{-}pydc)_4(H_2O)_6]_n$, there are two 2,4-pydc, a Cu^{2+} ion and a Gd^{3+} ion in its asymmetric unit. Two

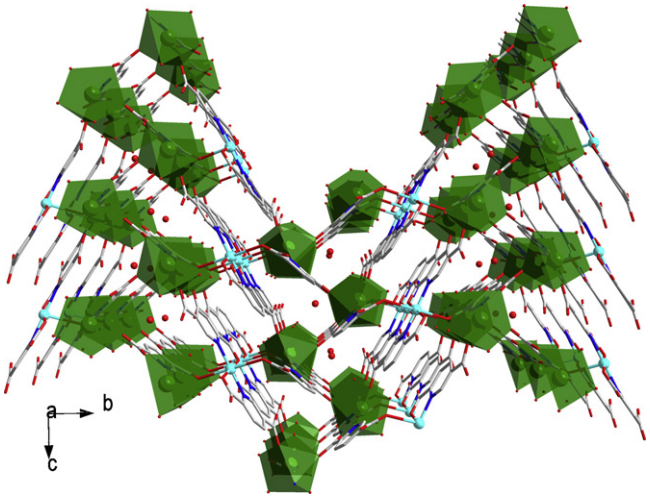

Fig. 17. The 3D structure of $[\{Ln_4Cu_2(2,5\text{-pydc})_8(H_2O)_{12}\}\cdot 4H_2O]_n$ [74b].

2,4-pydc anions chelate the Cu^{2+} ion forming a $[Cu(2,4\text{-pydc})_2]^{2-}$ subunit. The Gd^{3+} ions are connected by 2,4-pydc anions leading to a layer. Finally, the $[Cu(2,4\text{-pydc})_2]^{2-}$ subunits pillar the layers generating a 3D structure. $[Ln_2Cu_3(2,4\text{-pydc})_6(H_2O)_6]_n$ also can be considered as 2,4-pydc ligands pillaring carboxyl-bridged layers. For the Tb^{3+} derivative, a possible antiferromagnetic interaction between metal ions was observed. Unexpectedly, for the Er^{3+} derivative, the χT vs T curve increases slightly from 300–326 K and then decreases rapidly, suggesting effective ferromagnetic interaction between metal ions. Furthermore, the M–H curve and the nonzero imaginary component χ'' below 10 K confirmed a ferromagnetic interaction. Using 2,5-H_2pydc, we also synthesized a 3D structure formulated as $[\{Ln_4Cu_2(2,5\text{-pydc})_8(H_2O)_{12}\}\cdot 4H_2O]_n$ (Ln = Sm, Gd, Er). In this compound, the Ln^{3+} ions are first linked together giving rise to a wave-like layer structure with carboxylate-bridged Ln^{3+} chains [74b]. Two 2,5-pydc dianions chelate one Cu^{2+} ion using its pyridine N atom and one of their 2-carboxylate O atoms forming $[Cu(2,5\text{-pydc})_2]^{2-}$ subunit. The $[Cu(2,5\text{-pydc})_2]^{2-}$ subunits further pillar the wave-like layers leading to the 3D structure (Fig. 17). Temperature dependence of magnetic susceptibilities of the Gd^{3+} and Er^{3+} derivatives was measured from 300 to 2 K. Fitting the results with Curie-Weiss law generated the θ value of −0.29 and −4.81, respectively, showing a weak antiferromagnetic interaction between metal ions. In addition, Yue and coworkers presented a similar structure formulated as $[Gd_2Cu(2,5\text{-pydc})_2(CO_3)_2(H_2O)_2]\cdot 2H_2O$ constructed from $[Cu(2,5\text{-pydc})_2]^{2-}$ bridges pillared $\{[Gd_2(CO_3)_2]^{2+}\}_n$ sheets [95].

Another important type of 3D Ln–TM structures is a porous framework with 1D channels. The combination of effective magnetic coupling between metal ions and the porous character makes them good candidates for magnetic adsorption materials. Employing pyridine carboxylate ligands such as 2,3-H_2pydc, 2,6-H_2pydc and pyridine 2,4,6-tricarboxylic acids (2,4,6-H_3pytc), several compounds belonging to this type have been obtained generally under hydrothermal condition. Hydrothermal reaction of $LnCl_3\cdot 6H_2O$ (Ln = Gd, Dy), $M(NO_3)_3\cdot 6H_2O$ (M = Co, Ni) and 2,3-H_2pydc resulted in a 3D porous framework with 1D chair-like channels along c axis formulated as $[Ln_2(H_2O)_4M_2(H_2O)_2(2,3\text{-pydc})_5]\cdot nH_2O$ [8]. Because of the spin-orbital coupling of the metals in the system, it is difficult to determine the magnetic nature between the Ln^{3+} and TM^{3+} ions. However, the χT vs T curves with negative θ values indicate possible antiferromagnetic interactions in all compounds of this system. Employing 2,6-H_2pydc, a hexagonal 3D Ln–TM coordination polymer feature as nanotubular structure with formula $[\{[Ln(2,6\text{-pydc})_3Mn_{1.5}(H_2O)_3]\cdot nH_2O\}_\infty]$ (Ln = Pr, Gd, Er, Eu),was obtained [4,7]. In this system, each Mn^{2+} ion connects to four Ln^{3+} ions through the carboxylate groups from 2,6-pydc ligands in planar geometry and each Ln^{3+} ion connects to six Mn^{2+} ions, resulting in the porous 3D structure with hexagonal nanotubular channels. From the view of topology, this structure can be simplified as (4, 6) connected net with $((4^4\cdot 6^2)(4^9\cdot 6^6))$ Schläfli symbol. Unfortunately, the nature of the magnetic interaction for the Pr, Er, and Eu derivatives was not determined. For the Gd derivative, the coupling between Gd^{3+} and Mn^{2+} ions seems to be antiferromagnetic. Interestingly, the Eu derivative can be applied as a luminescent probe for Zn^{2+} ions. Porous Ln–TM compounds constructed from 2,4,6-H_3pytc have also been reported. For example, Tong and coworkers obtained a system of 3D Ln–Co porous magnets exhibiting selective gas adsorption behavior with formula $[Ln_4Co_3(pyta)_6(H_2O)_9]\cdot 5H_2O$ (Ln = Sm, Eu, Gd) [96]. Compared with the unclear magnetic nature for the Sm, Eu derivatives, the overall ferromagnetic interactions between adjacent Gd···Gd and Gd···Co centers were confirmed by the χT vs T curve for the Gd derivative.

3.5.2. Materials based on mixed cooperative ligands

As bridging ligands, pyridine carboxylic acids have shown their great ability to construct 3D Ln–TM compounds. If a second ligand were to be introduced, the cooperativity of both bridging ligands may lead to new open frameworks. Oxalic acid and 1,2-benzenedicarboxylic acid (H_2bdc), due to their various coordination modes and chelating coordination, have been widely employed by Yang et al. to construct 3D Ln–TM compounds with diverse topologies. The synthesis strategy of employing two different pyridine carboxylic acids has also proven to be effective.

Yang and coworkers reported two 3D Ln–TM compounds based on the cooperation of oxalic acid and pyridine carboxylic acids with formulae $[Ln(in)(C_2O_4)(H_2O)_2]$ (Ln = La, Pr, Nd) and $LnCu(na)_2(C_2O_4)\cdot 1.5H_2O$ (Ln = La, Ce) [97]. The first one exhibits a 3D uninodal 8-connected framework with a unique $3^6\cdot 4^{18}\cdot 5^3\cdot 6$ topology. In this compound, two crystallographically identical Ln^{3+} ions are linked by four ina ligands to give a dinuclear unit, and then each dinuclear unit was bridged by four oxalate ligands to give (4, 4) net, which are further extended by the bridging $Cu(ina)_2^-$ to give a 3D network. Treating the dinuclear unit as a node, this network can be viewed as an 8-connected net. For the second compound, the na ligand was obtained from the decarboxylation of 2,3-H_2pydc and it exhibit a rarely reported eight-connected self-penetrating ilc net with dinuclear $\{Ln_2\}$ subunits as secondary building units. Four na^- and four oxalate ligands link two Ln^{3+} ions to form $\{Ln_2\}$ subunits which are extended by oxalate ligands leading to a 2D (4, 4) layer. Linear $Cu(na)_2^-$ anions further link the layers into the finial 3D network. No magnetic properties measurement was carried out for either compound.

Several 3D Ln–Cu compounds based on the cooperation of H_2bdc and pyridine carboxylic acids are available in the literature. Generally, these structures have pillars supporting layer topologies, the linear $Cu(ina)_2^-$ anions acting as pillars. However the layer substructures are diverse, including layers of $\{Ln_{36}\}$ wheels, bdc^{2-} ligands linked Ln–organic layer and bdc^{2-} cooperation with ina linked Ln–organic layers. As an impressive example, Yang and coworkers reported a Ln–Cu sandwich framework comprising $\{Cu_3\}$ cluster pillars and a layered network of $\{Er_{36}\}$ wheels with formula $[Er_7(\mu_3\text{-}O)(\mu_3\text{-}OH)_6(bdc)_3](ina)_9[Cu_3X_4]$ (X = Cl or Br) (Fig. 18) [73b]. In this surprising structure, the Er^{3+} ions are linked by hydroxo and oxo bridges to give two types of small cluster cores: cubic $[Er_4(\mu_3\text{-}O)(\mu_3\text{-}OH)_3]^{7+}$, {Er4} core, and dimeric $[Er_2(\mu_3\text{-}OH)_2]^{4+}$, $\{Er_2\}$ core. The $\{Er_4\}$ cores link alternately the $\{Er_2\}$ cores to form a nanosized $\{Er_{36}\}$ wheel with an 18-ring. Each $\{Er_{36}\}$ wheel is linked to surrounding wheels to form a layered network with honeycomb arrays. On the other hand, three Cu ions are bridged by μ-Cl atoms to form a $\{Cu_3Cl_4\}$ trimeric

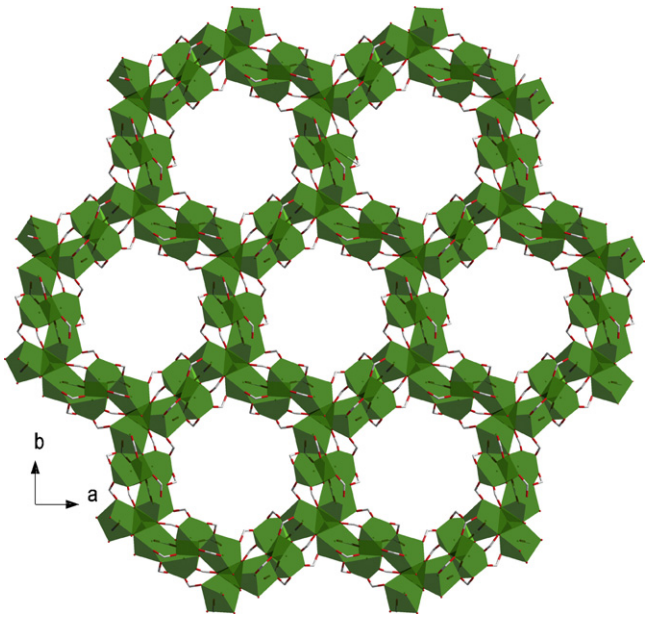

Fig. 18. The layer of $\{Er_{36}\}$ wheels in $[Er_7(\mu_3\text{-}O)(\mu_3\text{-}OH)_6(bdc)_3](ina)_9[Cu_3X_4]$ [73b].

cluster, which links six ina ligands to form a new pillar supporting the layers of $\{Er_{36}\}$ wheels. As the temperature is lowered, this compound shows a continuous decrease in μ_{eff}, this behavior may be attributed to the crystal-field splitting of the Er^{3+} ion and the contribution of overall antiferromagnetic interactions. Unfortunately, no magnetic ordering and frequency dependence were observed above 2 K. Two further 3D Ln–Cu compounds with pillared topologies with formulae $Ln_2(bdc)_2(ina)_2(H_2O)_2Cu{\cdot}X$ (Ln = Eu, Sm, Nd, X = Cl^- or ClO_4^-) and $[Er_4(ina)_8(bdc)_2(OH){\cdot}(H_2O)_5][Cu_8I_7]$ were reported [98]. In the first compound, the linear $Cu(ina)_2^-$ anions act as pillars linking the Ln-bdc layers together to result in 3D framework as a (5,6)-connected net with $(4^7{\cdot}6^3)(4^7{\cdot}6^8)$ Schläfli symbol. For the second compound, chains of $[Cu_8I_7]_n^{n+}$ clusters pillar the Er-organic layers to form a 3D structure. Different from the two compounds above, another 3D Ln–Cu compound with formula $[Ce_3(ina)_8(bdc)(H_2O)_4][Cu_7Br_6]$ contains a 1D $[Cu_6Br_6]_n$ chainlike motif inserted into the channels of its 3D framework [98a].

New products will be obtained if an additional, different, pyridine carboxylic acid is added to the reaction system. Indeed, several new 3D Ln–TM compounds were synthesized with this strategy. A 3D Ln–Cu compound $[Ce_2(ina)_5(na)_2(H_2O)_2][Cu_5Br_4]$ constructed from interlinked Ce–organic double chains and inorganic $[Cu_5Br_4]_n^{n+}$ chains was synthesized by Yang and coworkers [98a]. Based on three different pyridine carboxylate acids, they obtained a 3D compound $Er_4(OH)_4Cu_5I_4(ina)_6(na)(2,5\text{-}pydc){\cdot}0.3H_2O$, which is constructed from decanuclear $[Cu_{10}I_8]^{2+}$ clusters and inorganic 1D $[Er_4(OH)_4]_n^{8n+}$ cluster chain-based layers. The na^- in the compound was from the decarboxylation of $2,5\text{-}pydc^{2-}$ [93b]. In addition, they reported a 3D Ln–TM compound $Ln_2Cu_2I_2(OH)_2(pca)_2(na)_2$ (Ln = Y, Er, Yb) using the cooperation of pca and na ligands. This compound is constructed from two distinct second building units (SBUs) of cubane $\{Ln_4\}$ and chair-like $\{Cu_4\}$ clusters, resulting in a 3D framework with an unusual bimodal (6, 8)-connected net [99]. The magnetic properties for these complexes were not reported.

No Ln–TM compound constructed solely from 3,4-H_2pydc has been reported. While employing the cooperation of 3,4-H_2pydc and na, a 3D Ln–Ag compound $LnAg(pydc)_2(na)_{0.5}$ (Ln = Nd, Eu) was obtained [100]. The Ag^+ and Ln^{3+} ions are first linked to form 1D inorganic heterometallic chains which are further linked by pydc ligands into a 3D open framework. A few, 3D Ln–TM compounds constructed from the cooperation of pyridine carboxylic acids with other bridging ligands (such as 4,4′-bipy, glycol, azido) have also been reported. For example, Bu et al. obtained a 3D framework $[GdNi_2(ina)_5(N_3)_2(H_2O)_3]{\cdot}2H_2O$ constructed from antiferromagnetic azido-bridged Ni^{2+} chains and ferromagnetic carboxylate-bridged Gd^{3+} chains; while Cheng and coworkers reported a 3D Pr/Ni/Na heterotrimetallic framework $\{Na_2NiPr(\mu_4\text{-}ClO_4)(\mu_2\text{-}HOCH_2CH_2OH)(\mu_4\text{-}2,4,6\text{-}pytc)_2(H_2O)_8\}{\cdot}4.5H_2O\}_n$ containing four different bridging ligands [101].

4. Conclusion remarks

A variety of Ln–TM hybrid materials with diverse structures has been synthesized. These structures not only enrich the database of topologies but also supply excellent models for studying magnetic interactions involving lanthanide and transition metal ions. Furthermore, some of these materials exhibit novel magnetic properties such as magnetic ordering and slow relaxation, which entitle them to be good candidates for future magnetic materials. Further with the development of Ln–TM hybrid materials, some new synthesis strategies have been proposed.

However, due to the orbital contribution of lanthanide ions, which introduces many complications, in particular large magnetic anisotropies, the understanding of the magnetic interactions involving lanthanide ions in molecular magnets is still far from being satisfactory. It is still necessary to gather more experimental data about this issue. The availability of sophisticated physical measurements and computational methods has dramatically improved the development of magnetic chemistry, so a clear view of the magnetic interactions involving lanthanide ions can be expected.

Although a few Ln–TM compounds showing slow relaxation have been synthesized, their block temperatures (T_b) are all too low to be applied. The number of the Ln–TM materials exhibiting long-range order is also limited but with the improvement of synthesis strategies and measurements, more Ln–TM materials with improved magnetic properties will be synthesized in the near future.

Acknowledgements

This work was supported by grants of the National Natural Science Foundation of China and the Natural Science Foundation of Fujian Province and The Young Scientist Funds of Fujian Province (Nos. 2006F3130 and 2006F3138).

References

[1] (a) C. James, P.S. Willand, J. Am. Chem. Soc. 38 (1916) 1497;
(b) W.E. Bailey, R.J. Williams, W.O. Milligan, Acta Crystallogr. B29 (1973) 1365;
(c) J.M. Boncella, R.A. Andersen, Inorg. Chem. 23 (1984) 432;
(d) A. Figuerola, C. Diaz, J. Ribas, V. Tangoulis, J. Granell, F. Lloret, J. Mahia, M. Maestro, Inorg. Chem. 42 (2003) 641;
(e) B. Yang, Z. Chen, Prog. Nat. Sci. 11 (2001) 401.
[2] (a) C.E. Plečnik, S. liu, S.G. Shore, Acc. Chem. Res. 36 (2003) 499;
(b) C.M. Zaleski, E.C. Depperman, J.W. Kampf, M.L. Kirk, V.L. Pecoraro, Inorg. Chem. 45 (2006) 10022;
(c) C. Aronica, G. Pilet, G. Chastanet, W. Wernsdorfer, J.F. Jacquot, D. Luneau, Angew. Chem. Int. Ed. 45 (2006) 4659.
[3] (a) M.C. Hong, Cryst. Growth Des. 7 (2007) 10;
(b) S. Osa, T. Kido, N. Matsumoto, N. Re, A. Pochaba, J. Mrozinski, J. Am. Chem. Soc. 126 (2004) 420;
(c) C.M. Zaleski, E.C. Depperman, J.W. Kampf, M.L. Kirk, V.L. Pecoraro, Angew. Chem. Int. Ed. 43 (2004) 3912;
(d) H.Z. Kou, Y.B. Jiang, A.L. Cui, Cryst. Growth Des. 5 (2005) 77;
(e) S.M. Hu, J.C. Dai, X.T. Wu, L.M. Wu, C.P. Cui, Z.Y. Fu, M.C. Hong, Y.C. Liang, J. Cluster Sci. 13 (2002) 33.
[4] (a) B. Zhao, X.Y. Chen, P. Cheng, D.Z. Liao, S.P. Yan, Z.H. Jiang, J. Am. Chem. Soc. 126 (2004) 15394;
(b) B. Zhao, H.L. Gao, X.Y. Chen, P. Cheng, W. Shi, D.Z. Liao, S.P. Yan, Z.H. Jiang, Chem. Eur. J. 12 (2006) 149.
[5] (a) A. Rath, E. Aceves, J. Mitome, J. Liu, U.S. Ozkan, S.G. Shore, J. Mol. Catal. A: Chem. 165 (2001) 103;
(b) S.G. Shore, E.R. Ding, C. Park, M.A. Keane, Catal. Commun. 3 (2002) 77;

(c) H.C. Aspinall, Chem. Rev. 102 (2002) 1807;
(d) M. Shibasaki, N. Yoshikawa, Chem. Rev. 102 (2002) 2187;
(e) J. Inanaga, H. Furuno, T. Hayano, Chem. Rev. 102 (2002) 2211.
[6] F. Luo, S.R. Batten, Y. Che, J.M. Zheng, Chem. Eur. J. 13 (2007) 4948.
[7] B. Zhao, P. Cheng, Y. Dai, C. Cheng, D.Z. Liao, S.P. Yan, Z.H. Jiang, G.L. Wang, Angew. Chem. Int. Ed. 42 (2003) 934.
[8] Q. Yue, J. Yang, G.H. Li, G.D. Li, W. Xu, J.S. Chen, S.N. Wang, Inorg. Chem. 44 (2005) 5241.
[9] (a) S. Tanase, J. Reedijk, Coord. Chem. Rev. 250 (2006) 2501;
(b) J.J. Attema, G.A. de Wijs, G.R. Blake, R.A. de Groot, J. Am. Chem. Soc. 127 (2005) 16325.
[10] (a) H.O. Stumpf, L. Ouahab, Y. Pei, P. Bergerat, O. Kahn, J. Am. Chem. Soc. 116 (1994) 3866;
(b) E. Coronada, C.J. Gómez-García, Chem. Rev. 98 (1998) 273;
(c) B.Q. Ma, S. Gao, G. Su, G.X. Xu, Angew. Chem. Int. Ed. 40 (2001) 434.
[11] (a) D.M.J. Doble, C.H. Benison, A.J. Blake, D. Fenske, M.S. Jackson, R.D. Kay, W.S. Li, M. Schröder, Angew. Chem. Int. Ed. 38 (1999) 1915;
(b) J. Lisowski, P. Starynowicz, Inorg. Chem. 38 (1999) 1351;
(c) J. Liu, E.A. Meyers, J.A. Cowan, S.G. Shore, Chem. Commun. (1998) 2043;
(d) G.B. Deacon, C.M. Forsyth, T. Behrsing, K. Konstas, M. Forsyth, Chem. Commun. (2002) 2820.
[12] (a) C. Benelli, A. Caneschi, D. Gatteschi, O. Guillou, L. Pardi, Inorg. Chem. 29 (1990) 1750;
(b) M. Andruh, I. Ramade, E. Codjovi, O. Guillou, O. Kahn, J.C. Trombe, J. Am. Chem. Soc. 115 (1993) 1822;
(c) A. Bencini, C. Benelli, A. Caneschi, A. Dei, D. Gatteschi, Inorg. Chem. 25 (1986) 572;
(d) C. Aronica, G. Chastanet, G. Pilet, B.L. Guennic, V. Robert, W. Wernsdorfer, D. Luneau, Inorg. Chem. 46 (2007) 6108.
[13] (a) F. Mori, T. Nyui, T. Ishida, T. Nogami, K.Y. Choi, H. Nojiri, J. Am. Chem. Soc. 128 (2006) 1440;
(b) J. Paulovic, F. Cimpoesu, M. Ferbinteanu, K. Hirao, J. Am. Chem. Soc. 126 (2004) 3321.
[14] J.P. Hay, J.C. Thibeault, R. Hoffmann, J. Am. Chem. Soc. 97 (1975) 4884.
[15] P.W. Anderson, Solid State Phys. 14 (1963) 99.
[16] P. de Loth, P. Cassoux, J.P. Daudey, J.P. Malrieu, J. Am. Chem. Soc. 103 (1981) 4007.
[17] L. Noodleman, C.Y. Peng, D.A. Case, J.M. Mouesca, Coord. Chem. Rev. 144 (1995) 199.
[18] R. Caballol, O. Castell, F. Illas, I.P.R. Moreira, J.P. Malrieu, J. Phys. Chem. A 101 (1997) 7860.
[19] C. Adamo, V. Barone, A. Bencini, F. Totti, I. Ciofini, Inorg. Chem. 38 (1999) 1996.
[20] (a) E. Juiz, J. Cano, S. Alvarez, P. Alemany, J. Am. Chem. Soc. 120 (1998) 11122;
(b) A. Bencini, C. Benelli, A. Caneschi, A. Dei, D. Gatteschi, Inorg. Chem. 25 (1986) 572.
[21] A. Bencini, C. Benelli, A. Caneschi, R.L. Carlin, A. Dei, D. Gatteschi, J. Am. Chem. Soc. 107 (1985) 8128.
[22] Y. Pei, Y. Journaux, O. Kahn, A. Dei, D. Gatteschi, J. Chem. Soc., Chem. Commun. (1986) 1300.
[23] C. Benelli, A. Caneschi, D. Gatteschi, O. Guillou, L. Pardi, Inorg. Chem. 29 (1990) 1750.
[24] M. Sakamoto, M. Hashimura, K. Matsuki, N. Matsumato, K. Inoue, H. Okawa, Bull. Chem. Soc. Jpn. 64 (1991) 3639.
[25] D.M.L. Goodgame, D.J. Williams, R.E.P. Winpenny, Polyhedron 8 (1989) 1531.
[26] S. Wang, Z. Pang, M.J. Wagner, Inorg. Chem. 31 (1992) 5381.
[27] A.J. Blake, P.E.Y. Milne, R.E.P. Winpenny, P. Thornton, Angew. Chem. Int. Ed. 30 (1991) 1139.
[28] A.J. Blake, R.O. Gould, P.E.Y. Milne, R.E.P. Winpenny, J. Chem. Soc., Chem. Commun. (1991) 1453.
[29] (a) C.M. Zaleski, E.C. Depperman, J.W. Kampf, M.L. Kirk, V.L. Pecoraro, Angew. Chem. Int. Ed. 43 (2004) 3912;
(b) F. Pointillart, K. Bernot, R. Sessoli, D. Gatteschi, Chem. Eur. J. 13 (2007) 1602;
(c) V.M. Mereacre, A.M. Ako, R. Clériac, W. Wernsdorfer, G. Filoti, J. Bartolomé, C.E. Anson, A.K. Powell, J. Am. Chem. Soc. 129 (2007) 9248;
(d) A. Mishra, W. Wernsdorfer, K.A. Abboud, G. Christou, J. Am. Chem. Soc. 126 (2004) 15648;
(e) M. Murugesu, A. Mishra, W. Wernsdorfer, K.A. Abboud, G. Christou, Polyhedron 25 (2006) 613;
(f) A. Mishra, W. Wernsdorfer, S. Parsons, G. Christou, E.K. Brechin, Chem. Commun. (2005) 2086;
(g) V. Ereacre, A.M. Ako, R.R. Clérac, W. Wernsdorfer, I.J. Hewitt, C.E. Anson, A.K. Powell, Chem. Eur. J. 14 (2008) 3577;
(h) T.C. Stamatatos, S.J. Teat, W. Wernsdorfer, G. Christou, Angew. Chem. Int. Ed. 48 (2009) 521.
[30] F. Hulliger, M. Landolt, H. Vetsch, J. Solid State Chem. 18 (1976) 283.
[31] G.M. Li, T. Akitsu, O. Sato, Y. Einaga, J. Am. Chem. Soc. 125 (2003) 12396.
[32] (a) X.M. Chen, Y.Y. Yang, Chin. J. Chem. 18 (2000) 664;
(b) N. Sakagami, K. Okamoto, Chem. Lett. (1998) 201;
(c) S. Decurtins, M. Gross, H.W. Schmalle, S. Ferlay, Inorg. Chem. 37 (1998) 2443;
(d) A.D. Cutland, R.G. Malkani, J.W. Kampf, V.L. Pecoraro, Angew. Chem. Int. Ed. 39 (2000) 2689;
(e) M.L. Kahn, M. Verelst, M. Lecante, C. Mathonière, O. Kahn, Eur. J. Inorg. Chem. (1999) 527;
(f) T. Sanada, T. Suzuki, S. Kaizaki, J. Chem. Soc. Dalton Trans. (1998) 959.
[33] (a) O. Guillou, O. Kahn, R.L. Oushoorn, K. Boubekeur, P. Batail, Inorg. Chim. Acta 198 (1992) 119;
(b) O. Kahn, Y. Pei, M. Verdaguer, J.P. Renard, J. Sletten, J. Am. Chem. Soc. 110 (1988) 782;
(c) Y. Pei, M. Verdaguer, O. Kahn, J. Sletten, J.P. Renard, Inorg. Chem. 26 (1987) 138;
(d) M.L. Kahn, C. Mathoniere, O. Kahn, Inorg. Chem. 38 (1999) 3692.
[34] (a) Y.C. Liang, R. Cao, M.C. Hong, D.F. Sun, Y.J. Zhao, J.B. Weng, R.H. Wang, Inorg. Chem. Commun. 5 (2002) 366;
(b) D.F. Sun, R. Cao, Y.C. Liang, M.C. Hong, Chem. Lett. (2001) 878;
(c) Y.C. Liang, M.C. Hong, W.P. Su, R. Cao, W.J. Zhang, Inorg. Chem. 40 (2001) 4574;
(d) C. Benelli, D. Gatteschi, Chem. Rev. 102 (2002) 2369;
(e) E.P. Winpenny, Chem. Soc. Rev. 27 (1998) 447.
[35] (a) Y. Matuura, S. Matsushima, M. Sakamoto, Y. Sadaoka, J. Mater. Chem. 3 (1993) 767;
(b) M. Sakamoto, K. Matsuki, R. Ohsumi, Y. Nakayama, A. Matsumoto, H. Okawa, Bull. Chem. Soc. Jpn. 65 (1992) 2278;
(c) A. Rath, E. Aceves, J. Mitome, J. Liu, U.S. Ozkan, S.G. Shore, J. Mol. Catal. A: Chem. 165 (2001) 103;
(d) S.G. Shore, E.R. Ding, C. Park, M.A. Keane, Catal. Commun. 3 (2002) 77.
[36] (a) X.J. Kong, Y.P. Ren, L.S. Long, Z. Zheng, R.B. Huang, L.S. Zheng, J. Am. Chem. Soc. 129 (2007) 7016;
(b) M. Shibasaki, N. Yoshikawa, Chem. Rev. 102 (2002) 2187.
[37] (a) H.C. Aspinall, Chem. Rev. 102 (2002) 1807;
(b) J. Lisowski, P. Starynowicz, Inorg. Chem. 38 (1999) 1351.
[38] (a) G.B. Deacon, C.M. Forsyth, T. Behrsing, K. Konstas, M. Forsyth, Chem. Commun. (2002) 2820;
(b) J. Liu, E.A. Meyers, J.A. Cowan, S.G. Shore, Chem. Commun. (1998) 2043.
[39] X.M. Chen, Y.L. Wu, Y.Y. Yang, S.M.J. Aubin, D.N. Hendrickson, Inorg. Chem. 37 (1998) 6186.
[40] Y. Cui, G. Cheng, J. Ren, Y.T. Qian, J.S. Huang, Inorg. Chem. 39 (2000) 4165.
[41] K. Harada, J. Yuzurihara, Y. Ishii, N. Sato, H. Kambayashi, Y. Fukuda, Chem. Lett. (1995) 887.
[42] Y.Y. Yang, Y.L. Wu, L.S. Long, X.M. Chen, J. Chem. Soc. Dalton Trans. (1999) 2005.
[43] M. Sassaki, K. Manseki, H. Horiuchi, M. Kumagai, M. Sakamoto, H. Sakiyama, Y. Nishida, Y. Sadaoka, M. Ohba, H. Okawa, J. Chem. Soc. Dalton Trans. (2000) 259.
[44] (a) J.P. Costes, F. Dahan, A. Dupuis, J.P. Laurent, Inorg. Chem. 36 (1997) 4284;
(b) J.L. Sanz, R. Ruiz, A. Gleizes, F. Lloret, J. Faus, M. Julve, J.J. Borras-Almenar, Y. Journaux, Inorg. Chem. 35 (1996) 7384;
(c) J.P. Costes, F. Dahan, A. Dupuis, J.P. Laurent, Chem. Eur. J. 4 (1998) 1616.
[45] J.P. Costes, F. Dahan, A. Dupuis, J.P. Laurent, New J. Chem. 22 (1998) 1525.
[46] C. Brewer, G. Brewer, W.R. Scheidt, M. Shang, E.E. Carpenter, Inorg. Chim. Acta 313 (2001) 65.
[47] C. Benelli, A.J. Blake, P.E.Y. Milne, J.M. Rawson, R.E.P. Winpenny, Chem. Eur. J. 1 (1995) 614.
[48] (a) A.J. Blake, R.O. Gould, P.E.Y. Milne, R.E.P. Winpenny, J. Chem. Soc., Chem. Commun. (1992) 522;
(b) A.J. Blake, P.E.Y. Milne, R.E.P. Winpenny, P. Thornton, Angew. Chem. Int. Ed. 30 (1991) 1139.
[49] A.J. Blake, P.E.Y. Milne, R.E.P. Winpenny, J. Chem. Soc. Dalton Trans. (1993) 3727.
[50] Y. Yukawa, S. Igarashi, A. Yamano, S. Sato, Chem. Commun. (1997) 711.
[51] S.-M. Hu, J.C. Dai, X.T. Wu, L.M. Wu, C.P. Cui, Z.Y. Fu, M.C. Hong, Y.C. Liang, J. Cluster Sci. 13 (2002) 33.
[52] J.J. Zhang, S.M. Hu, L.M. Zheng, X.T. Wu, Z.Y. Fu, J.C. Dai, W.X. Du, H.H. Zhang, R.Q. Sun, Chem. Eur. J. 8 (2002) 5742.
[53] (a) F. Avecilla, C. Platas-Iglesias, R. Rodriguez-Cortinas, G. Guillemot, J.C.G. Bunzli, C.D. Brondino, C.F.G.C. Geraldes, A. de Blas, T. Rodriguez-Blas, J. Chem. Soc. Dalton Trans. (2002) 4658;
(b) J.P. Costes, F. Dahan, G. Novitchi, V. Arion, S. Shova, J. Lipkowski, Eur. J. Inorg. Chem. (2004) 1530;
(c) G. Novitchi, S. Shova, A. Caneschi, J.P. Costes, M. Gdaniec, N. Stanica, Dalton Trans. (2004) 1194.
[54] J.P. Costes, F. Dahan, A. Dupuis, Inorg. Chem. 39 (2000) 165.
[55] A.J. Stemmler, J.W. Kampf, M.L. Kirk, B.H. Atasi, V.L. Pecoraro, Inorg. Chem. 38 (1999) 2807.
[56] Q.Y. Chen, Q.H. Luo, L.M. Zheng, Z.L. Wang, J.T. Chen, Inorg. Chem. 41 (2002) 605.
[57] J.P. Costes, F. Dahan, A. Dupuis, J.P. Laurent, C. R. Acad. Sci. Paris, Ser. IIc (1998) 417.
[58] T. Sanada, T. Suzuki, T. Yoshida, S. Kaizaki, Inorg. Chem. 37 (1998) 4712.
[59] J.P. Costes, F. Dahan, A. Dupuis, L.P. Laurent, Inorg. Chem. 39 (2000) 169.
[60] A.J. Blake, R.O. Gould, C.M. Grant, P.E.Y. Milne, S. Parsons, R.E.P. Winpenny, Dalton Trans. (1997) 485.
[61] (a) X.M. Chen, S.M.J. Aubin, Y.L. Wu, Y.S. Yang, T.C.W. Mak, D.N. Hendrickson, J. Am. Chem. Soc. 117 (1995) 9600;
(b) X.M. Chen, Y.L. Wu, Y.X. Tong, X.Y. Huang, J. Chem. Soc. Dalton Trans. (1996) 2443.
[62] (a) J.J. Zhang, T.L. Sheng, S.Q. Xia, G. Leibeling, F. Meyer, S.M. Hu, R.B. Fu, S.C. Xiang, X.T. Wu, Inorg. Chem. 43 (2004) 5472;
(b) J.J. Zhang, S.C. Xiang, S.M. Hu, S.Q. Xia, R.B. Fu, X.T. Wu, Y.M. Li, H.S. Zhang, Polyhedron 23 (2004) 2265;
(c) J.J. Zhang, S.M. Hu, L.M. Zheng, X.T. Wu, Z.Y. Fu, J.C. Dai, W.X. Du, H.H. Zhang, R.Q. Sun, Chem. Eur. J. 8 (2002) 5742;

(d) S.C. Xiang, S.M. Hu, T.L. Sheng, R.B. Fu, X.T. Wu, X.D. Zhang, J. Am. Chem. Soc. 129 (2007) 15144.
[63] Q.D. Liu, S. Gao, J.R. Li, Q.Z. Zhou, K.B. Yu, B.Q. Ma, S.W. Zhang, X.X. Zhang, T.Z. Jin, Inorg. Chem. 39 (2000) 2488.
[64] J.J. Zhang, S.Q. Xia, T.L. Sheng, S.M. Hu, G. Leibeling, F. Meyer, X.T. Wu, S.C. Xiang, R.B. Fu, Chem. Commun. (2004) 1186.
[65] X.J. Kong, Y.P. Ren, W.X. Chen, L.S. Long, Z.P. Zheng, R.B. Huang, L.S. Zheng, Angew. Chem. Int. Ed. 47 (2008) 2398.
[66] (a) O. Kahn, Acc. Chem. Res. 33 (2000) 647;
(b) K.M. Dunbar, R.A. Heintz, Prog. Inorg. Chem. 36 (1997) 283.
[67] B. Zhao, P. Cheng, Y. Dai, C. Cheng, D.Z. Liao, S.P. Yan, Z.H. Jiang, G.L. Wang, Angew. Chem. Int. Ed. 42 (2003) 934.
[68] R. Gheorghe, P. Cucos, M. Andruh, J.P. Costes, B. Donnadieu, S. Shova, Chem. Eur. J. 12 (2006) 187.
[69] T.k. Prasad, M.V. Rajasekharan, J.P. Costes, Angew. Chem. Int. Ed. 46 (2007) 2851.
[70] (a) J.J. Zhang, T.L. Sheng, S.M. Hu, S.Q. Xia, G. Leibeling, F. Meyer, Z.Y. Fu, L. Chen, X.T. Wu, R.B. Fu, Chem. Eur. J. 10 (2004) 3963;
(b) F. He, M.L. Tong, X.L. Yu, X.M. Chen, Inorg. Chem. 44 (2005) 559.
[71] (a) Z. He, C. He, E.Q. Gao, Z.M. Wang, X.F. Yang, C.S. Liao, C.H. Yan, Inorg. Chem. 42 (2003) 2206;
(b) A.Q. Wu, G.H. Guo, C. Yang, F.K. Zheng, X. Liu, G.C. Guo, J.S. Huang, Z.C. Dong, Y. Takano, Eur. J. Inorg. Chem. (2005) 1947.
[72] O. Guillou, P. Bergerat, O. Kahn, E. Bakalbassis, K. Boubekeur, P. Batail, M. Guillot, Inorg. Chem. 31 (1992) 110.
[73] (a) J.W. Cheng, J. Zhang, S.T. Zheng, G.Y. Yang, Chem. Eur. J. 14 (2008) 88;
(b) J.W. Cheng, J. Zhang, S.T. Zheng, M.B. Zhang, G.Y. Yang, Angew. Chem. Int. Ed. 45 (2006) 73.
[74] (a) Y.C. Liang, R. Cao, W.P. Su, M.C. Hong, Chem. Lett. (2000) 868;
(b) Y.C. Liang, R. Cao, W.P. Su, M.C. Hong, W.J. Zhang, Angew. Chem. Int. Ed. 39 (2000) 3304;
(c) Y.C. Liang, M.C. Hong, R. Cao, W.P. Su, Y.J. Zhao, J.B. Weng, R.G. Xiong, Bull. Chem. Soc. Jpn. 75 (2002) 1521;
(d) Y.F. Zhou, F.L. Jiang, D.Q. Yuan, B.L. Wu, R.H. Wang, Z.Z. Lin, M.C. Hong, Angew. Chem. Int. Ed. 43 (2004) 5665;
(e) Y.G. Huang, M.Y. Wu, W. Wei, Q. Gao, D.Q. Yuan, F.L. Jiang, M.C. Hong, J. Mol Struct. 885 (2008) 23;
(f) Y.G. Huang, M.Y. Wu, F.Y. Lian, F.L. Jiang, M.C. Hong, Inorg. Chem. Commun. 11 (2008) 840;
(g) Y.G. Huang, X.T. Wang, F.L. Jiang, S. Gao, M.Y. Wu, Q. Gao, W. Wei, M.C. Hong, Chem. Eur. J. 14 (2008) 10340.
[75] (a) F.A. Cotton, C. Lin, C.A. Murillo, Acc. Chem. Res. 34 (2001) 759;
(b) M. Eddaoudi, D.B. Moler, H. Li, B. Chen, T.M. Reineke, M. O'keeffe, O.M. Yaghi, Acc. Chem. Res. 34 (2001) 319.
[76] X.N. Cheng, W.X. Zhang, Y.Y. Lin, Y.Z. Zheng, X.M. Chen, Adv. Mater. 19 (2007) 2843.
[77] (a) B. Yan, H.D. Wang, Z.D. Chen, Inorg. Chem. Commun. 3 (2000) 653;
(b) B. Yan, Z. Chen, Chem. Lett. (2000) 1244;
(c) B. Yan, Z. Chen, S. Wang, S. Gao, Chem. Lett. (2001) 350;
(d) A. Figuerola, C. Diaz, M.S. El Fallah, J. Ribas, M. Maestro, J. Mahia, Chem. Commun. (2001) 1204.
[78] (a) J. Legendziewicz, M. Borzechowska, G. Oczko, G. Meyer, New J. Chem. 24 (2000) 53;
(b) Y.P. Cai, C.Y. Su, G.B. Li, Z.W. Mao, C. Zhang, A.W. Xu, B.S. Kang, Inorg. Chem. Acta 358 (2005) 1298;
(c) S. Decurtins, M. Gross, H.W. Schmalle, S. Ferlay, Inorg. Chem. 37 (1998) 2443.
[79] (a) M.L. Kahn, C. Mathoniere, O. Kahn, Inorg. Chem. 38 (1999) 3692;
(b) M.L. Kahn, P. Lecante, M. Verelst, C. Mathoniere, O. Kahn, Chem. Mater. 12 (2000) 3073;
(c) M.L. Kahn, M. Verelst, P. Lecante, C. Mathoniere, O. Kahn, Eur. J. Inorg. Chem. (1999) 527.
[80] (a) R.L. Oushoorn, K. Boubekeur, P. Batail, O. Guillou, O. Kahn, Bull. Soc. Chim. Fr. 133 (1996) 777;
(b) O. Guillou, O. Kahn, R.L. Oushoorn, K. Boubekeur, P. Batail, Inorg. Chim. Acta 198 (1992) 119;
(c) O. Guillou, R.L. Oushoom, O. Kahn, K. Boubekeur, P. Batail, Angew. Chem. Int. Ed. 31 (1992) 626.
[81] (a) H.Z. Kou, S. Gao, X.L. Jin, Inorg. Chem. 40 (2001) 6295;
(b) H.Z. Kou, S. Gao, B.W. Sun, J. Zhang, Chem. Mater. 13 (2001) 1431.
[82] B.Q. Ma, S. Gao, G. Su, G.X. Xu, Angew. Chem. Int. Ed. 40 (2001) 434.
[83] (a) W.F. Yeung, T.C. Lau, X.Y. Wang, S. Gao, L. Szeto, W.T. Wong, Inorg. Chem. 45 (2006) 6756;
(b) J.M. Herrera, S.G. Baca, H. Adams, M.D. Ward, Polyhedron 25 (2006) 869;
(c) T. Hozumi, S.I. Ohkoshi, Y. Arimoto, H. Seino, Y. Mizobe, K. Hashimoto, J. Phys. Chem. B 107 (2003) 11571.
[84] (a) P. Mahata, G. Sankar, G. Madras, S. Natarajan, Chem. Commun. (2005) 5787;
(b) J.W. Wu, J.F. Yin, T.W. Tseng, K.L. Lu, Inorg. Chem. Commun. 11 (2008) 314.
[85] (a) F.Q. Wang, X.J. Zheng, Y.H. Wan, C.Y. Sun, Z.M. Wang, K.Z. Wang, L.P. Jin, Inorg. Chem. 46 (2007) 2956;
(b) C. Daigubonne, O. Guillou, M.L. Kahn, O. Kahn, R.L. Oushoorn, K. Boubekeur, Inorg. Chem. 40 (2001) 176.
[86] F. Hulliger, M. Landolt, H. Vetsch, J. Solid State Chem. 18 (1976) 283.
[87] (a) A.C. Rizzi, R. Calvo, R. Baggio, M.T. Garland, O. Pena, M. Perec, Inorg. Chem. 41 (2001) 5609;
(b) R. Baggio, M.T. Garland, Y. Moreno, O. Pena, M. Perec, E. Spodine, J. Chem. Soc. Dalton Trans. (2000) 2061.
[88] Q.D. Liu, J.R. Li, S. Gao, B.Q. Ma, F.H. Liao, Q.Z. Zhou, K.B. Yu, Inorg. Chem. Commun. 4 (2001) 301.
[89] (a) C. Livage, N. Guillou, J. Marrot, G. Frey, Chem. Mater. 13 (2001) 4387;
(b) B.L. Chen, N.W. Ockwig, F.R. Fronczek, D.S. Contreras, O.M. Yaghi, Inorg. Chem. 44 (2005) 181.
[90] X.J. Gu, D.F. Xue, Cryst. Growth Des. 7 (2007) (1726).
[91] M.B. Zhang, J. Zhang, S.T. Zheng, G.Y. Yang, Angew. Chem. Int. Ed. 44 (2005) 1385.
[92] F. Luo, Y.X. Che, J.M. Zheng, Cryst. Growth Des. 6 (2006) 2432.
[93] (a) X.J. Gu, D.F. Xue, Inorg. Chem. 46 (2007) 5349;
(b) J.W. Cheng, S.T. Zheng, G.Y. Yang, Inorg. Chem. 47 (2008) 4930.
[94] F. Luo, D.X. Hu, L. Xue, Y.X. Che, J.M. Zheng, Cryst. Growth Des. 7 (2007) 851.
[95] N. Wang, S.T. Yue, Y.L. Liu, H.Y. Yang, H.Y. Wu, Cryst. Growth Des. 9 (2009) 368.
[96] C.J. Li, Z.J. Lin, M.X. Peng, J.D. Leng, M.M. Yang, M.L. Tong, Chem. Commun. (2008) 6348.
[97] (a) J.W. Cheng, S.T. Zheng, G.Y. Yang, Dalton Trans. (2007) 4059;
(b) J.W. Cheng, S.T. Zheng, W. Liu, G.Y. Yang, CrystEngComm 10 (2008) 765.
[98] (a) J.W. Cheng, S.T. Zheng, G.Y. Yang, Inorg. Chem. 46 (2007) 10261;
(b) J.W. Cheng, S.T. Zheng, E. Ma, G.Y. Yang, Inorg. Chem. 46 (2007) 10534.
[99] J.W. Cheng, S.T. Zheng, W. Liu, G.Y. Yang, CrystEngComm 10 (2008) 1047.
[100] X.J. Gu, D.F. Xue, CrystEngComm 9 (2007) 471.
[101] (a) H.L. Gao, L. Yi, B. Ding, H.S. Wang, P. Cheng, D.Z. Liao, S.P. Yan, Inorg. Chem. 45 (2006) 481;
(b) F.C. Liu, Y.F. Zeng, J. Jiao, J.R. Li, X.H. Bu, J. Ribas, S.R. Batten, Inorg. Chem. 45 (2006) 6129.